BAMS Article

Challenges and Opportunities Offered by Geostationary Space Observations for Air Quality Research and Emission Monitoring

Tai-Long He,[a,b] Glenn-Michael Oomen,[c] Wenfu Tang,[h] Idir Bouarar,[d] Kelly Chance,[e] Cathy Clerbaux,[f,g] David P. Edwards,[h] Henk Eskes,[i] Benjamin Gaubert,[h] Claire Granier,[j,k,l] Marc Guevara,[m] Daniel J. Jacob,[b] Jennifer Kaiser,[n,o] Jhoon Kim,[p] Shobha Kondragunta,[q] Xiong Liu,[e] Eloise A. Marais,[r] Kazuyuki Miyazaki,[s] Rokjin Park,[t] Vincent-Henri Peuch,[u] Gabriele Pfister,[h] Andreas Richter,[v] Trissevgeni Stavrakou,[c] Raid M. Suleiman,[e] Alexander J. Turner,[a] Ben Veihelmann,[w] Zhao-Cheng Zeng,[x] and Guy P. Brasseur[d]

KEYWORDS: Remote sensing; Satellite observations; Forecasting; Air pollution; Air quality; Atmospheric composition

ABSTRACT: Space-borne remote sensing of atmospheric chemical constituents is crucial for monitoring and better understanding global and regional air quality. Since the 1990s, the continuous development of instruments onboard low-Earth orbiting (LEO) satellites has led to major advances in air quality research by providing daily global measurements of atmospheric chemical species. The next generation of atmospheric composition satellites measures from the geostationary Earth orbit (GEO) with hourly temporal resolution, allowing the observation of diurnal variations of air pollutants. The first two instruments of the GEO constellation coordinated by the Committee on Earth Observation Satellites (CEOS), the Geostationary Environment Monitoring Spectrometer (GEMS) for Asia and the Tropospheric Emissions: Monitoring of Pollution (TEMPO) for North America, were successfully launched in 2020 and 2023, respectively. The European component, Sentinel-4, is planned for launch in 2025. This work provides an overview of satellite missions for atmospheric composition monitoring and the state of the science in air quality research. We cover recent advances in retrieval algorithms, the modeling of emissions and atmospheric chemistry, data assimilation, and the application of machine learning based on satellite data. We discuss the challenges and opportunities in air quality research in the era of GEO satellites and provide recommendations on research priorities for the near future.

SIGNIFICANCE STATEMENT: Space-borne measurements of the chemical composition of the atmosphere are crucial for understanding and forecasting air quality. With the next generation of atmospheric composition satellites measuring from the geostationary Earth orbit, air quality research has entered a new era. We provide an overview of the constellation of satellites for atmospheric composition monitoring and review the latest advances in satellite-driven air quality research. We identify the challenges and opportunities for a better exploitation of the wealth of satellite data from a geostationary perspective.

DOI: 10.1175/BAMS-D-23-0145.1

Corresponding authors: Tai-Long He, the@g.harvard.edu; Glenn-Michael Oomen, glenn-michael.oomen@aeronomie.be
Tai-Long He and Glenn-Michael Oomen contributed equally to this work.

Publisher's Note: This article was revised on 10 June to update the acknowledgments.

Manuscript received 13 June 2023, in final form 3 January 2025, accepted 9 January 2025

AFFILIATIONS: [a] Department of Atmospheric and Climate Science, University of Washington, Seattle, Washington; [b] John A. Paulson School of Engineering and Applied Sciences, Harvard University, Cambridge, Massachusetts; [c] Royal Belgian Institute for Space Aeronomy (BIRA-IASB), Brussels, Belgium; [d] Max Planck Institute for Meteorology, Hamburg, Germany; [e] Center for Astrophysics, Harvard & Smithsonian, Cambridge, Massachusetts; [f] LATMOS/IPSL, Sorbonne Université, UVSQ, CNRS, Paris, France; [g] Spectroscopy, Quantum Chemistry and Atmospheric Remote Sensing (SQUARES), Université libre de Bruxelles, Brussels, Belgium; [h] Atmospheric Chemistry Observations & Modeling Laboratory, NSF National Center for Atmospheric Research, Boulder, Colorado; [i] Royal Netherlands Meteorological Institute, De Bilt, Netherlands; [j] Laboratoire d'Aérologie, Université de Toulouse, CNRS, UPS, Toulouse, France; [k] NOAA Chemical Sciences Laboratory, Boulder, Colorado; [l] CIRES, University of Colorado Boulder, Boulder, Colorado; [m] Barcelona Supercomputing Center, Barcelona, Spain; [n] School of Civil and Environmental Engineering, Georgia Institute of Technology, Atlanta, Georgia; [o] School of Earth and Atmospheric Sciences, Georgia Institute of Technology, Atlanta, Georgia; [p] Department of Atmospheric Sciences, Yonsei University, Seoul, South Korea; [q] NOAA/NESDIS, College Park, Maryland; [r] Department of Geography, University College London, London, United Kingdom; [s] Jet Propulsion Laboratory, California Institute for Technology, Pasadena, California; [t] School of Earth and Environmental Sciences, Seoul National University, Seoul, South Korea; [u] European Centre for Medium-Range Weather Forecasts, Reading, United Kingdom; [v] Institute of Environmental Physics, University of Bremen, Bremen, Germany; [w] ESA-ESTEC, Noordwijk, Netherlands; [x] School of Earth and Space Sciences, Peking University, Beijing, China

1. Introduction

Air pollution is one of the leading causes of global premature mortality and economic damages (Cohen et al. 2017; Dechezleprêtre et al. 2019). Space-borne remote sensing instruments have played a key role in monitoring atmospheric composition since the 1990s (Burrows et al. 1999; Bovensmann et al. 1999; Drummond and Mand 1996; Veefkind et al. 2006, 2012; Zoogman et al. 2017; Levelt et al. 2018; Kim et al. 2020, among others). Satellite observations have been used with sophisticated models to help develop policies to reduce emissions (e.g., Duncan et al. 2016; Jiang et al. 2018), improve our knowledge about air pollution (e.g., Fu et al. 2007; Silvern et al. 2019; Yang et al. 2023b), and better forecast air quality (e.g., Peuch et al. 2022; Eskes et al. 2024). Efficient reduction of air pollution often contributes to the reduction of co-emitted greenhouse gases (GHGs) and toward the mitigation of climate change (West et al. 2013; Miyazaki and Bowman 2023).

Efforts have been made to improve the observation of atmospheric composition from space over the past two decades. The Tropospheric Monitoring Instrument (TROPOMI; 2017–the present; Veefkind et al. 2012) is the first to provide daily global multiconstituent measurements at a sub-10-km spatial resolution (Veefkind et al. 2012), which helps to reveal detailed linkages between human activities and air quality (e.g., Riess et al. 2022; Martínez-Alonso et al. 2023; Zuo et al. 2023). The next generation of atmospheric composition monitoring satellites measures column abundances of trace gases from the geostationary Earth orbit (GEO). The first two GEO atmospheric composition satellites, Geostationary Environment Monitoring Spectrometer (GEMS; Kim et al. 2020) for Asia and Tropospheric Emissions: Monitoring of Pollution (TEMPO; Zoogman et al. 2017) for North America, were successfully launched in 2020 and 2023, respectively. The European component, Sentinel-4, is planned for launch in 2025 (Stark et al. 2013). Ongoing low-Earth orbiting (LEO) missions have been proposed to sustain atmospheric composition observations outside the GEO domains.

The International Space Science Institute (ISSI) offers the platform to facilitate international collaboration on interdisciplinary research in space science. The ISSI International Expert Team 489 (Brasseur and Granier 2020) recently assessed advancements in the use of space-borne instruments to improve air quality characterization and forecasts. We summarize the discussion and conclusions from the ISSI Team 489 Workshop (2023) in this paper to provide an overview of the opportunities and challenges arising in the era of GEO atmospheric composition satellites. The recently launched and scheduled satellite instruments motivate us to review the state of air quality research based on satellite observations. We cover advances in the development of retrieval algorithms, modeling, and forecasting of air quality, data assimilation, and machine learning applications. We conclude with recommendations for research priorities for the near future to better exploit GEO satellite atmospheric composition observations.

2. Constellation of LEO and GEO atmospheric composition satellites

a. Heritage of LEO satellites. Column concentrations of short-lived air pollutants, including tropospheric ozone (O_3), nitrogen dioxide (NO_2), sulfur dioxide (SO_2), formaldehyde (HCHO), and aerosols, are retrieved in the ultraviolet (UV), visible (Vis), and near-infrared

Table 1. Constellation of nadir-viewing LEO and GEO space-borne atmospheric chemistry monitoring instruments since 2000. Instruments dedicated to measuring GHGs are not considered within the scope of the paper. The asterisk symbol denotes (*) IASI and IASI-NG have a circular pixel geometry of 12-km diameter. The double asterisk symbol denotes ** AMI, AGRI, AHI, and ABI have pixel sizes from 0.5 × 0.5 km² to 1 × 1 km² for Vis bands and 2 × 2 km² for IR bands at nadir. The triple asterisk symbol denotes * ABI, AHI, and AMI scan the full disk of observational coverage every 10 min. AGRI scans the full disk every 15 min. All three instruments support regional scans at 5 min or higher frequencies. The quadruple asterisk symbol denotes **** GOCI-2 scans northeast Asia hourly and scans the full disk of East Asia, Southeast Asia, and Oceania once per day. The quintuple asterisk symbol denotes ***** IRS scans Europe every 30 min and scans the full disk of Europe and Africa once per hour. The sextuple asterisk symbol denotes ****** GXI will be on the GeoXO East and GeoXO West platforms to be launched in 2032 and 2035, respectively. ACX and GXS will be hosted on the GeoXO Central platform scheduled for launch in 2035. The septuple asterisk symbol denotes ******* GXS scans the full disk of observational coverage every 30 min. It can also scan the contiguous United States every 15 min or scan mesoscale regions every 5 min. GXI will have the same overall scan rates as GOES ABI.**

Satellite	Instrument	Operation period	Spectral range	Resolution (km²)	Coverage[a]	Overpass time (local)	Covered region
			LEO				
ERS-2	GOME	1995–2011	UV–Vis	40 × 320	3 days	1030	Global
Envisat	SCIAMACHY	2002–12	UV–Vis–SWIR	30 × 60	6 days	1000	
Aqua	AIRS	2002–the present	TIR	13.5 × 13.5	0.5 day	0130/1330	
Terra	MOPITT	1999–the present	NIR–TIR	22 × 22	5 days	1030/2230	
MetOp	GOME-2	2006–the present	UV–Vis	40 × 80	1.5 days	0930	
	IASI		TIR	12 × 12*	0.5 day	0930/2130	
Aura	OMI	2004–the present	UV–Vis	13 × 24	1 day[b]	1345	
JPSS[c]	OMPS	2012–the present	UV–Vis	10 × 10[d]	1 day	1330	
	CrIS		TIR	14 × 14	0.5 day	0130/1330	
Sentinel-5P	TROPOMI	2017–the present	UV–Vis–NIR–SWIR	3.5 × 5.5[e]	1 day	1330	
Fengyun-3[f]	HIRAS	2019–the present	TIR	14 × 14	0.5 day	See footnote f	
MetOp SG A	IASI-NG	*2025*	TIR	12 × 12*	0.5 day	0930/2130	
	Sentinel-5		UV–Vis–NIR–SWIR	7 × 7	1 day	0930	

(*Continued*)

Table 1. Continued.

Satellite	Instrument	Operation period	Spectral range	Resolution (km²)	Coverage[a]	Overpass time (local)	Covered region
			GEO				
GK-2A	AMI	2018–the present	Vis–IR	2 × 2 at nadir**	10 min***	Continuous	East Asia, Southeast Asia, and Oceania
GK-2B	GEMS	2020–the present	UV–Vis	3.5 × 7.7 at 37.5°N	1 h		East Asia
	GOCI-2		UV–NIR	2.5 × 2.5 at equator	1 h****		Northeast Asia and the full disk****
Intelsat 40e	TEMPO	2023–the present	UV–Vis	2.0 × 4.75 at 33.7°N	1 h		North America
MTG-S	Sentinel-4	*2025*	UV–Vis–NIR	8 × 8 at 45°N	1 h		Europe and North Africa
	IRS		TIR	4 × 4 at nadir	1 h*****		Europe and Africa*****
Himawari-8/9	AHI	2015–the present	Vis–IR	2 × 2 at nadir**	10 min***		East Asia, Southeast Asia, and Oceania
Fengyun-4	AGRI	2016–the present	Vis–IR	2 × 2 at nadir**	15 min***		Asia, Southeast Asia, and Oceania
	GIIRS		TIR	12 × 12 at nadir[g]	1.5 h[h]		East Asia
GOES[i]	ABI	2017–the present	Vis–IR	2 × 2 at nadir**	10 min***		Western Hemisphere
GeoXO******	ACX	*2035******	UV–Vis	8 × 3 at nadir	1 h		North America
	GXS		TIR	4 × 4 at nadir	30 min*******		Western Hemisphere
	GXI	*2032******	Vis–IR	1 × 1 at nadir[j]	10 min*******		Western Hemisphere

[a] Time required for global coverage for LEO instruments or coverage of the field of regard for GEO instruments.
[b] The revisit time of OMI was increased to 2–3 days since 2018 due to the OMI row anomaly (Torres et al. 2018).
[c] CrIS and OMPS are currently on the *Suomi NPP*, *NOAA-20*, and *NOAA-21* satellites. They will also fly on the JPSS-3 and JPSS-4 satellites.
[d] Pixel size of OMPS nadir mapper (NM) on *Suomi NPP* is 50 × 50 km² but improved to 17 × 13 km² on *NOAA-20* and then 10 × 10 km² on *NOAA-21*. OMPS nadir profiler has 250 × 250 km² resolution.
[e] Resolution of TROPOMI at nadir observations was increased from 3.5 × 7 km² to 3.5 × 5.5 km² on 6 Aug 2019.
[f] HIRAS is currently on the *FY-3D*, *FY-3E*, and *FY-3F* satellites. The overpass times are 0200/1400 and 0530/1730 local time for *FY-3D* and FY-3E and 1000/2200 local time for *FY-3F*.
[g] Pixel size is 16 × 16 km² for GIIRS on *Fengyun-4A* and is 12 × 12 km² for GIIRS on *Fengyun-4B.*
[h] Time required to scan the field of regard is 2 h for GIIRS on *Fengyun-4A* and is 1.5 h for GIIRS on *Fengyun-4B*.
[i] ABI is now available on *GOES-16*, *GOES-17*, *GOES-18*, and *GOES-19*.
[j] Several Vis bands on GXI have 0.5 × 0.5 km² pixels at nadir, and the red band (0.64 μm) has 0.25 × 0.25 km² pixels at nadir. The IR bands on GXI will have resolutions of 1 × 1 km² and 2 × 2 km².

(NIR) spectral bands from nadir-viewing satellite instruments. NASA's backscatter UV (BUV) instruments were the first satellite missions measuring total ozone columns since the 1970s (Mateer et al. 1971; Heath et al. 1975; Frederick et al. 1986; Bhartia et al. 2013). As shown in Table 1, satellites in LEO provide a nearly daily global coverage, and their spatial resolution has improved over time. Compared to Global Ozone Monitoring Experiment (GOME) (1995–2011; Burrows et al. 1999), the GOME-2 series (2006–the present; Munro et al. 2016) measure at 4 times higher spatial resolution, and the Ozone Monitoring

Instrument (OMI; 2004–the present; Veefkind et al. 2006) has a further improved spatial resolution (13 × 24 km^2). Measurements made by GOME, GOME-2, SCIAMACHY (2002–12; Bovensmann et al. 1999), and OMI include important chemical species for atmospheric chemistry and have greatly advanced our understanding of air quality (e.g., Duncan et al. 2016; Levelt et al. 2018). TROPOMI (2017–the present) onboard the Copernicus *Sentinel-5 Precursor* (*Sentinel-5P*) mission measures from UV–Vis–NIR to shortwave infrared (SWIR), which allows the measurements of an extended list of trace gases (Veefkind et al. 2012). Its unprecedented resolution of 3.5 × 5.5 km^2 and the high signal-to-noise ratio reveal enriched details of air pollution, which has greatly advanced air quality research in recent years (e.g., Fioletov et al. 2020; Stavrakou et al. 2020; Riess et al. 2022).

Infrared (IR) instruments also provide measurements about atmospheric composition. The Measurements of Pollution in the Troposphere (MOPITT; 1999–the present; Drummond et al. 2022; Buchholz et al. 2021) instrument measures carbon monoxide (CO) from the shortwave infrared and thermal infrared (TIR) and was one of the first satellite instruments that tracked global pollution transport. The Infrared Atmospheric Sounding Interferometer (IASI; 2006–the present; Clerbaux et al. 2009) instruments were launched on the Meteorological Operational satellites (MetOp) series, measuring meteorological variables, air pollutants, and greenhouse gases from the TIR with a 12-km footprint resolution. To date, 33 chemical species have been detected above the IASI instrumental noise level (Clarisse et al. 2011; Franco et al. 2018). As a companion to IASI, a series of TIR instruments have been launched by NASA and NOAA, the Atmospheric Infrared Sounder (AIRS; 2002–the present; Lambrigtsen et al. 2004) on *Aura* and NOAA's Cross-Track Infrared Sounder (CrIS; 2011–the present; Han et al. 2013).

Nadir-viewing LEO satellites provide valuable information on the seasonal and interannual variability of atmospheric composition. Rapid changes in emissions are detected, often in real time, as demonstrated during the lockdowns in response to the COVID-19 spread (Bauwens et al. 2020; F. Liu et al. 2020; Gkatzelis et al. 2021, among others). The LEO satellites provide decades of atmospheric composition measurements since the 1990s, allowing trend analysis at different spatial scales (e.g., Lamsal et al. 2015; Duncan et al. 2016; Stavrakou et al. 2018; Hedelius et al. 2021; Fortems-Cheiney et al. 2021).

b. GEO satellites for atmospheric chemistry. Atmospheric composition measurements from GEO satellites greatly expand the global observing system for air quality. They can provide continuous observations during daytime hours (24 h in the TIR). The geostationary orbit is 36 000 km from Earth, as compared to ~500 km for LEO, but the weaker photon flux is compensated by a long staring capability so that pixel sizes and precisions from LEO and GEO atmospheric composition instruments are comparable. The same suite of species observable from LEO is also observable from GEO but with much higher data density over the field of regard. The field of regard for a geostationary instrument can be as large as one-third of Earth, although smaller domains are used in the geostationary air quality constellation (see Fig. 1) to increase data density and achieve finer pixel resolution. Geostationary satellites observe from fixed longitudes in an equatorial plane, which means that they have highest resolution at the equator and limited observation capability for latitudes poleward of 60°.

The Geostationary Interferometric Infrared Sounder (GIIRS) onboard China's Fengyun-4 satellite series (*FY-4A/B*) is the first GEO hyperspectral infrared sounder. *FY-4A* and *FY-4B* currently operate at 86.5° and 105°E, respectively. The GIIRS observations cover most of East Asia with a focus on China, with a 2-h observing cycle. GIIRS measures at a 12-km spatial resolution at nadir and was recently used to retrieve ammonia (NH_3; Clarisse et al. 2021; Zeng et al. 2023b), CO (Zeng et al. 2023a), and formic acid (HCOOH; Zeng et al. 2024). The GIIRS onboard *FY-4B* (GIIRS/*FY-4B*; 2021–the present) demonstrates improved sensitivity, better spatial resolution, and higher accuracy compared to GIIRS/*FY-4A* (2016–the present; Yang

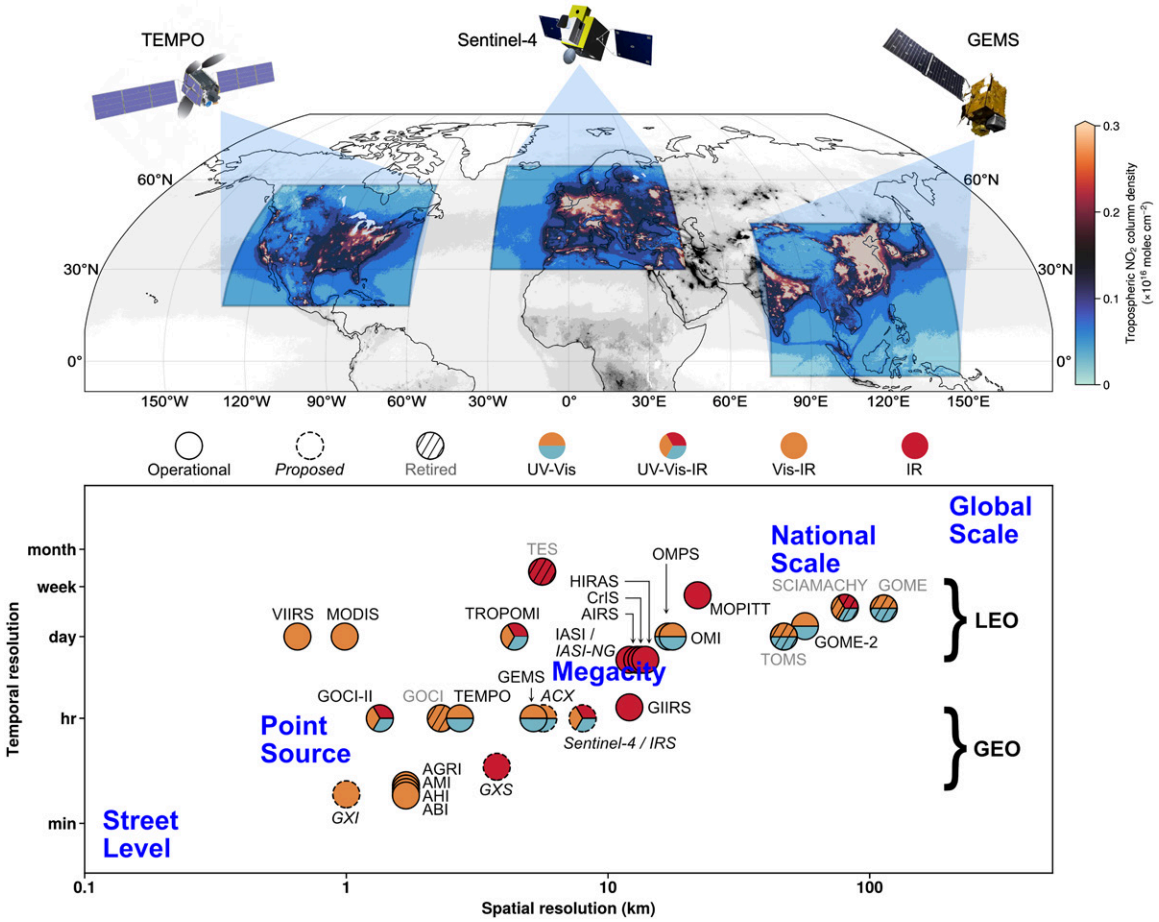

FIG. 1. (top) Domain and coverage of the GEO satellites. Background is annual-mean TROPOMI NO_2 tropospheric columns in 2022. Regions not covered by the GEO satellites are shaded in gray. (bottom) Spatial and temporal resolution of space-borne instruments for atmospheric composition measurements. Figure adapted from Fig. 1 in Kim et al. (2020).

et al. 2017). *FY-4A/B* also carry the Advanced Geosynchronous Radiation Imager (AGRI) that measures in Vis and IR.

GEMS is the first component of the GEO air quality constellation (see Fig. 1) and measures aerosols, O_3, NO_2, SO_2, HCHO, and glyoxal (CHOCHO), over Asia. It measures in UV–Vis with a spectral resolution of 0.6 nm and a spatial resolution of 3.5 km [north–south (NS)] × 7.7 km [east–west (EW)] at Seoul. It operates above 128.2°E, covering a field of regard from east of Japan to western India (75°–145°E) and from Mongolia to Indonesia (45°N–5°S). GEMS is the first satellite observing the diurnal variation of air pollution in Asia, including urban pollution, power plants, industrial activities, ship emissions, wildfires, Asian dust, and volcanic eruptions. Figure 2a shows tropospheric NO_2 columns measured by GEMS for July 2023. Asian megacities are observed as pollution hotspots. The diurnal column variations of tropospheric NO_2 columns in Seoul, Beijing, and New Delhi show large disparities due to regional differences in emissions, chemistry, and transport (see Fig. 2c).

NASA's first Earth Venture Instrument (EVI), TEMPO, is hosted onboard the Intelsat 40e satellite operating above 91°W. Compared to GEMS, TEMPO has a similar spectral resolution and an additional Vis–NIR channel to enhance retrieval sensitivity for tropospheric O_3 (Zoogman et al. 2017) and aerosols (X. Chen et al. 2021). TEMPO scans North America from east to west hourly with a spatial resolution of 2.0 km (NS) × 4.75 km (EW) at the center of the field of regard (see Fig. 2). TEMPO started its nominal operation in October 2023. The beta version of data products was released on NASA's Atmospheric Science Data Center (ASDC) in May 2024 and was upgraded to the provisional status in December 2024 (see Table 2).

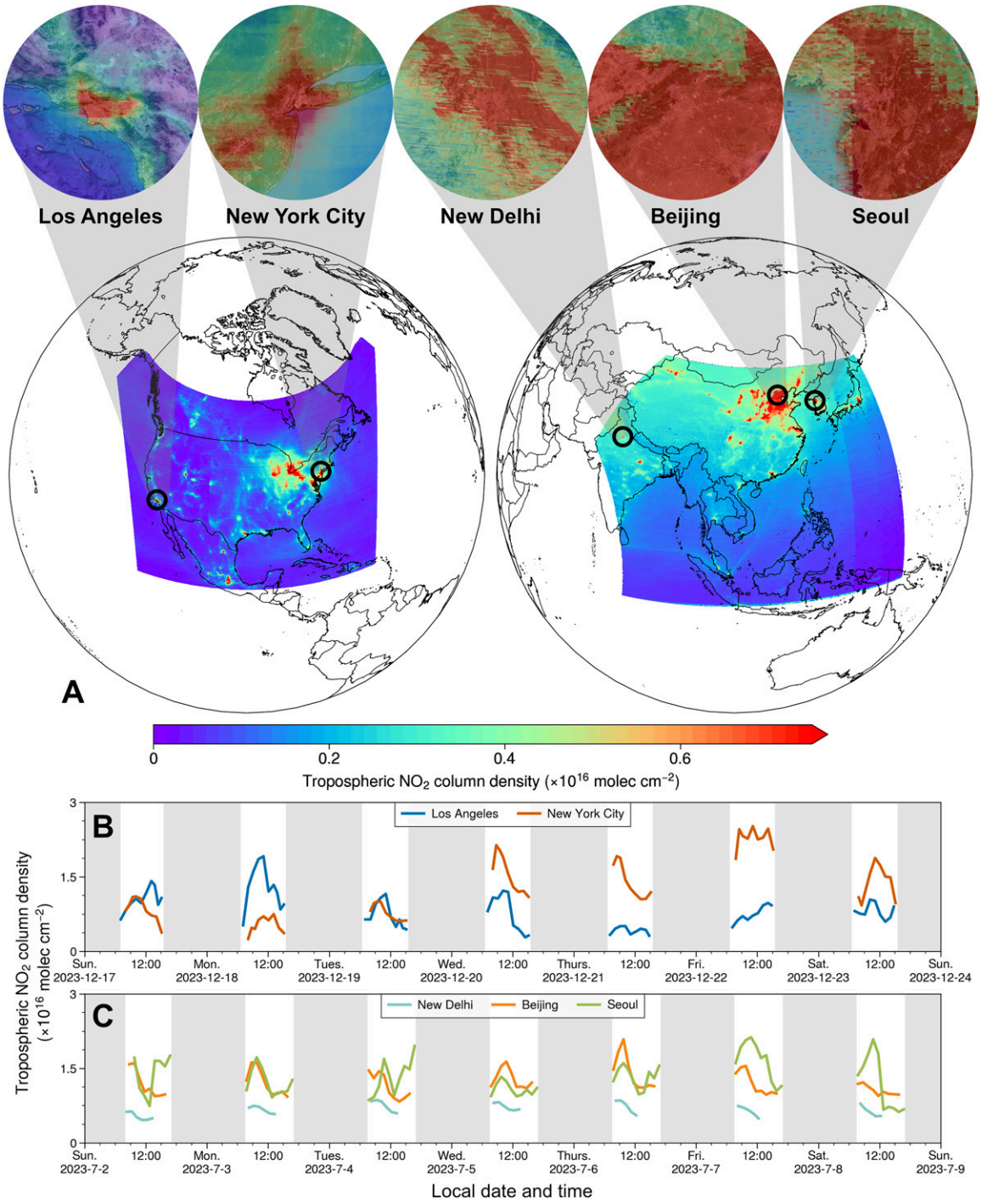

FIG. 2. (a) Illustration of tropospheric NO_2 column densities measured by (left) TEMPO and (right) GEMS. (top) Tropospheric NO_2 column densities measured over selected cities are shown. (b),(c) Hourly tropospheric NO_2 column density measurements show diurnal and weekly cycles over large cities. The TEMPO dataset used in this figure is preliminary and unvalidated and is used for illustration purposes only.

Figure 2 shows TEMPO tropospheric NO_2 columns with marked pollution hotspots including the Northeast corridor, the Canadian oil sands, and the Los Angeles basin. The observed diurnal variations of tropospheric NO_2 in New York City and Los Angeles for 17–24 December 2023 show large regional differences as seen by GEMS (see Fig. 2b). TEMPO can also measure the spectral signatures of nighttime lights and differentiate lighting types (Carr et al. 2017).

c. Future missions. The Copernicus Sentinel-4 mission will cover Europe, parts of North Africa, and parts of the Atlantic (see Fig. 1) centered at a fixed longitude of 0°, with an hourly

Table 2. Air pollutants retrieved from operational space-borne instruments, with DOIs to data products or references.

Instruments	NO_2	O_3	SO_2	VOC		Aerosols	HONO	CO	NH_3
				LEO					
TROPOMI	https://doi.org/10.5270/S5P-9bnp8q8	https://doi.org/10.5270/S5P-hcp1l2m	https://doi.org/10.5270/S5P-74eidii	HCHO	https://doi.org/10.5270/S5P-vg1i7t0	https://doi.org/10.5270/S5P-7g4iapn	https://doi.org/10.18758/71021058	https://doi.org/10.5270/S5P-bj3nry0	Not measured
				CHOCHO	https://doi.org/10.18758/4oaroxyf				
OMI	https://doi.org/10.5067/Aura/OMI/DATA2018	https://doi.org/10.5067/Aura/OMI/DATA2013	https://doi.org/10.5067/Aura/OMI/DATA2023	HCHO	https://doi.org/10.5067/Aura/OMI/DATA2015	https://doi.org/10.5067/Aura/OMI/DATA2001		Not measured	
GOME-2	Available at EUMETSAT Satellite Application Facility on Atmospheric Composition Monitoring (AC SAF)							Not measured	
IASI	Not measured	Available at AERIS atmospheric data center					https://doi.org/10.5281/zenodo.10721381	Available at AERIS	
OMPS	https://doi.org/10.5067/N0X-VLE2QAVR3	https://doi.org/10.5067/0WF4HAAZ0VHK	https://doi.org/10.5067/A9O02ZH0J94R	HCHO	https://doi.org/10.5067/IIM1GHT07QA8	https://doi.org/10.5067/40L92G8144IV		Not measured	
CrIS	Not measured	https://doi.org/10.5067/WUK-WENW76N5P	Hyman and Pavolonis (2020)	HCHO	Fu et al. (2019)	Not measured		https://doi.org/10.5067/BYIIUV3PR9L6	https://doi.org/10.5067/7I3KMUCCJNEN
Other LEO satellites	Not available	AIRS: https://doi.org/10.5067/Aqua/AIRS/DATA208	MLS: https://doi.org/10.5067/Aura/MLS/DATA2519	Not available		VIIRS: https://doi.org/10.5067/VIIRS/AERDB_L2_VIIRS_SNPP.002	Not available	MOPITT: https://doi.org/10.5067/TERRA/MOPITT/MOP03JM.009	AIRS: https://doi.org/10.5067/EYXLPVGTSWFF
				GEO					
GEMS	Available from NIER, ESC						Not available	Not measured	
TEMPO	https://doi.org/10.5067/IS-40e/TEMPO/NO2_L2.003	https://doi.org/10.5067/IS-40e/TEMPO/O3TOT_L2.003	Not available	HCHO	https://doi.org/10.5067/IS-40e/TEMPO/HCHO_L2.003	Not available		Not measured	
FY-4A/B (GIIRS)		Not measured		Not available		Available from Fengyun Data Center	Not measured	https://doi.org/10.18170/DVN/M7DKKL	https://doi.org/10.18170/DVN/VJ4MLO

measuring frequency similar to GEMS and TEMPO. The operational products include NO_2, O_3, SO_2, aerosols as well as the volatile organic compound (VOC) tracers HCHO and CHOCHO. The first Meteosat Third Generation Sounder (MTG-S1) satellite, expected to be launched in 2025, will carry a Sentinel-4 instrument on board as well as the Infrared Sounder (IRS) (Coopmann et al. 2023). The IRS has an observational coverage including the entire Africa and Europe. It will measure every 30 min above Europe and 1 h elsewhere in the field of regard, which could be useful for species with a strong diurnal variability such as NH_3 (see Clarisse et al. 2023).

The Geostationary Extended Observations (GeoXO) mission, NOAA's next-generation GEO constellation covering the Western Hemisphere, is scheduled for launch in the early 2030s (Lindsey et al. 2024). The central GeoXO platform (operating above ~105°W) will carry an atmospheric composition instrument (ACX) in the UV–Vis as well as a hyperspectral IR sounder (GXS) for measurements of CO, NH_3, isoprene, and other VOCs. The east and western GeoXO platforms will carry an imager (GXI) on board, similar to the *Geostationary Operational Environmental Satellite-16* (*GOES-16*) Advanced Baseline Imager (ABI) currently used in various applications. For example, Zhang et al. (2022) and O'Dell et al. (2024) estimated

surface particulate matter ($PM_{2.5}$) concentrations using aerosol optical depth measurements from *GOES-16* and *GOES-17*. Watine-Guiu et al. (2023) also showed the potential of using the GOES constellation to monitor methane point sources.

IASI–new generation (IASI-NG; Clerbaux and Crevoisier 2013; Crevoisier et al. 2014) is the follow-on program for IASI, which will be flown onboard the MetOp Second Generation (MetOp SG) satellites. The first MetOp SG platform is planned to be launched in 2025 to LEO and will also carry the Copernicus Sentinel-5 mission. IASI-NG will have higher spectral resolution and signal-to-noise ratio relative to IASI, providing better sensitivity near the surface and an improved vertical resolution of retrievals. Detection of weak absorbers (e.g., NH_3 and SO_2) will also improve.

3. Advances in air quality research using space-borne measurements

Over the past few decades, advances in atmospheric composition satellites have set the stage for air quality research and emission monitoring. The wealth of space observations has driven progress across all aspects of the research process. In this section, we provide an overview of recent advances in satellite-based air quality research. In section 3a, we review recent progress in the retrieval of atmospheric composition abundances from satellite measurements. In sections 3b and 3c, we introduce efforts to improve emission estimation and data assimilation techniques, respectively. Finally, in section 3d, we discuss the applications of machine learning in air quality research.

a. Improved retrieval algorithms. Technological innovations and increasing quality requirements are driving the science of satellite retrievals forward. For example, significant improvements have been made on retrieval algorithms for TROPOMI since its launch in 2017, with a focus on better constrained uncertainties and reduced biases (Theys et al. 2021; Heue et al. 2022; Van Geffen et al. 2022, among others). Besides an improved degradation correction (Ludewig et al. 2020) and better consistency among retrieval products (Tilstra et al. 2024), new retrievals from TROPOMI measurements were developed, e.g., solar-induced fluorescence (SIF; Guanter et al. 2021), aerosol optical depth (Torres et al. 2020), CHOCHO (Alvarado et al. 2020; Lerot et al. 2021), and nitrous acid (HONO; Theys et al. 2020). An overview of key air pollutants retrieved from space measurements is shown in Table 2.

The TROPOMI data products are carefully validated, and validation reports are released regularly. As such, TROPOMI has been used as the reference and transfer standard for the development of GEMS retrieval algorithms. The first evaluation of GEMS retrievals using TROPOMI and ground-based measurements showed a good consistency (Baek et al. 2023; Kim et al. 2023). GEMS measurements captured clear seasonal variations over cities as well as hourly variations that are also seen in ground-based remotely sensed columns (Lee et al. 2024). The list of GEMS retrievals was recently extended to SO_2 (Park and Jeong 2021), aerosols (Cho et al. 2024; Park et al. 2025), and glyoxal (Ha et al. 2024).

Continued efforts to improve retrieval algorithms have led to new data products for older missions like OMI, e.g., SO_2 (Li et al. 2022) and O_3 (Bak et al. 2024). Thermal infrared measurements are now better utilized to monitor extreme events, such as wildfires (Vu Van et al. 2023; Luo et al. 2024) and volcanic activities (Taylor et al. 2018). Notably, the phenomenal 2022 Hunga Tonga–Hunga Ha'apai eruption was well observed by thermal infrared spectrometers (e.g., Wright et al. 2022). The IASI NH_3 and ethylene (C_2H_4) retrievals were used to identify point sources from industrial and agricultural sectors (Van Damme et al. 2018; Franco et al. 2022).

The signal-to-noise ratio remains a limiting factor for the retrieval of weakly absorbing trace gases (e.g., formaldehyde, SO_2, and NH_3). Some recent studies average satellite measurements over longer time periods to obtain a significant signal (e.g., Van Damme et al. 2018). For more strongly absorbing gases, like NO_2, sources of retrieval uncertainties include

surface reflectivity, clouds and aerosols, and aspects like thermal contrast for infrared measurements. Atmospheric profiles have a strong impact on retrievals in the UV–Vis due to the altitude dependency of Rayleigh scattering, which becomes more important as the spatial resolution increases (Lamsal et al. 2021). Averaging kernels have been used in the validation of retrievals and data assimilation to account for the information content of the retrievals (Eskes and Boersma 2003).

To use satellite data at a higher spatial resolution, new oversampling methods have been developed (Valin et al. 2013; Fioletov et al. 2015; Sun et al. 2018; Van Damme et al. 2018; Clarisse et al. 2019, among others). For retrievals over emission hotspots, the assumptions about the vertical distribution of gases and their retrieval sensitivities (characterized by averaging kernels and airmass factors) are particularly important for the quantification of tropospheric amounts and diurnal variations (Yang et al. 2023b). Regional models capable of achieving 10-km resolution are being used to provide a priori information for high-resolution retrieval products [e.g., T. Liu et al. (2020) for NO_2 in Asia and Douros et al. (2023) for NO_2 in Europe].

b. Estimation of emissions. The development of emission inventories remains challenging due to the large number of species taken into account, the variety of emission sources, and because the a priori information is typically collected by networks that are spatially and temporally sparse (Granier et al. 2023; Sindelarova et al. 2023). For instance, the activity data and emission factors for anthropogenic emissions are available from diverse agencies, such as the International Energy Agency, but public access to this information is often limited. The development of open-source databases has been led by intergovernmental organizations, e.g., the Intergovernmental Panel on Climate Change Emissions Factor Database (IPCC EFDB) or the United Nations Framework Convention on Climate Change (UNFCCC), both of which are built on the data released in national reports. Global emission inventories are generally available with a delay of 3–4 years. To support policymaking and air quality applications, techniques have been developed to extrapolate emissions to the most recent years (Soulie et al. 2024). The development of emission inventories also needs to incorporate a finer temporal resolution and detailed categorization by specific emission sectors. To this end, temporal profiles based on statistical information (e.g., traffic counts) and meteorological parameterizations are typically considered (e.g., Guevara et al. 2021). Additional constraints on temporal profiles can be obtained from the hourly GEO observations, especially the diurnal variations of emissions (Park et al. 2024). Table 3 lists the main publicly available emission inventories, covering both pollutants and greenhouse gases at global and regional scales.

Large discrepancies have been highlighted among emission inventories due to differences in the activity data and emission factors (Elguindi et al. 2020; Granier et al. 2023). Complementary to the emission inventories, a growing number of studies (cf. section 3c) use satellite observations and inverse modeling techniques to estimate emissions, namely, NOx (e.g., Stavrakou et al. 2008; Kurokawa et al. 2009; Miyazaki et al. 2017; Jiang et al. 2022; Plauchu et al. 2024; van der A et al. 2024), VOCs (e.g., Millet et al. 2008; Stavrakou et al. 2012; Marais et al. 2012; Bauwens et al. 2016; Cao et al. 2018; Oomen et al. 2024; Müller et al. 2024), CO (e.g., Arellano et al. 2004; Müller et al. 2018; Qu et al. 2022b), and greenhouse gases (e.g., Wang et al. 2018; Lu et al. 2021). Figure 3 illustrates a comparison of NOx emissions in China from 2000 to 2020 from several emission inventories and satellite-based emission estimates (Elguindi et al. 2020). The differences between various estimates remain significant, especially for the trends, which underscores the need for continued efforts on mitigating uncertainties in emissions.

Table 3. List of several global and regional publicly available emissions inventories.

Acronym	Time period covered	Spatial resolution	Temporal resolution	Species considered	DOI or reference
			Global inventory		
EDGARv8	1970–2022	0.1° × 0.1°	Monthly	Pollutants + GHGs	Crippa et al. (2023a, 2024)
HTAPv3	2000–18	0.1° × 0.1°	Monthly	Pollutants	Crippa et al. (2023b)
CEDS	1980–2019	0.1° × 0.1°	Monthly	Pollutants + GHGs	https://www.pnnl.gov/projects/ceds
CAMS-GLOB-ANT v6.2	2000–25	0.1° × 0.1°	Monthly	Pollutants + GHGs	https://doi.org/10.24380/eets-qd81
ECLIPSE v6	1990–2050 (by 5 or 10 yrs)	0.5° × 0.5°	Yearly	Pollutants + CH_4	Klimont et al. (2017)
			Regional inventory		
CAMS-REG (Europe)	2000–22	0.1° × 0.05°	Yearly	Pollutants + GHGs	Kuenen et al. (2021)
EMEP (Europe)	1990–2022	No grid	Yearly	Pollutants	European Environment Agency (2023)
EPA[a] (United States)	1970–2023	No grid	Yearly	Pollutants + GHGs	epa.gov
Government Canada	1990–2022	No grid	Yearly	Pollutants + GHGs	Environment and Climate Change Canada (2019), Government of Canada (2018)
PAPILA (Latin America)	2014–20	0.1° × 0.1°	Yearly	Pollutants + GHGs	https://doi.org/10.5281/zenodo.12944491
DACCIWA (Africa)	1990–2015	0.1° × 0.1°	Yearly	Pollutants	Keita et al. (2021)
MIXv2 (Asia)	2010–17	0.1° × 0.1°	Monthly	Pollutants + CO_2	Li et al. (2024)
REASv3.2 (Asia)	1950–2015	0.25° × 0.25°	Monthly	Pollutants + CO_2	Kurokawa and Ohara (2020)
MEIC 1.4 (China)	1990–2020	0.25° × 0.25°	Monthly	Pollutants + CO_2	Zheng et al. (2018)

[a] Table shows the EPA Air Pollutant Emissions Trends Data. The EPA National Emissions Inventory (NEI) is available every 3 years with variable resolutions from 36 to 4 km.

The development of new retrievals (see section 3a) has advanced emission estimates from both natural and anthropogenic sources. For example, the new TROPOMI HONO retrieval product shows intense emissions in wildfire plumes, accounting for a substantial share of total hydroxyl radical (OH) production from natural sources (Theys et al. 2020). The first global satellite isoprene retrievals from CrIS (Fu et al. 2019), combined with HCHO observations, have been used to constrain isoprene emissions and atmospheric oxidation (Wells et al. 2020). These analyses reveal significantly underestimated isoprene emissions in emission inventories, particularly in tropical regions (Wells et al. 2020).

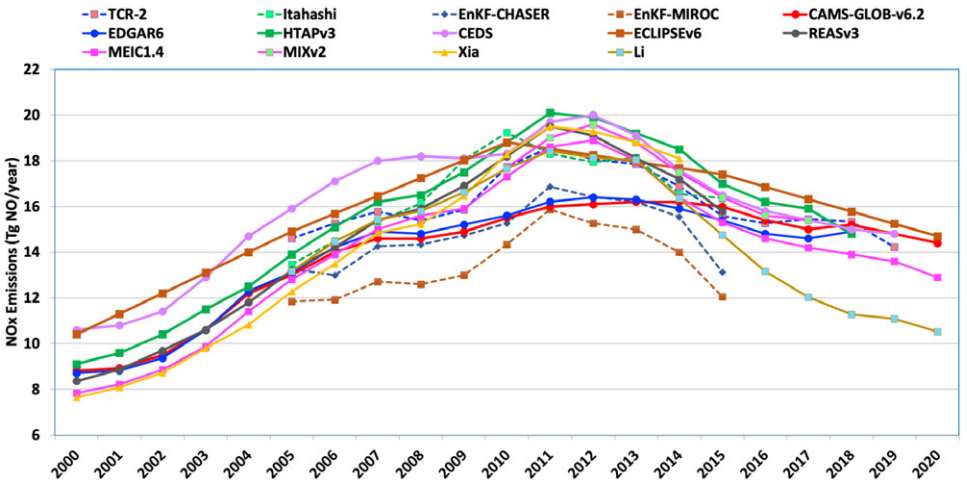

Fig. 3. Comparison of annual-mean NOx emissions in China from 2000 to 2020 (Tg NOx-NO/yr) from several datasets. Solid and dashed lines represent emission inventories and satellite-based emission estimates, respectively. (top) The references for the emission estimates are shown in the legend. Figure adapted from Elguindi et al. (2020).

The use of satellite retrievals has also proven to be crucial for identifying seasonalities and weekly patterns in emissions, providing complementary information to temporal profiles derived from activity data. This is particularly valuable for sources with limited activity information, such as those in the agricultural sector (e.g., Damme et al. 2022). Wind rotation method is another important advancement that estimates point source emissions by resolving emission plumes aligned with the wind direction (e.g., Beirle et al. 2011; Valin et al. 2013; Fioletov et al. 2015; Clarisse et al. 2019).

c. Advances in data assimilation. Data assimilation in air quality research combines observations with chemical transport models (CTMs) to produce an analysis of the state of atmospheric composition (e.g., Carmichael et al. 2008; Lahoz and Schneider 2014). Areas of application include air quality forecasting (e.g., Inness et al. 2015), inverse modeling of emissions and other model parameters, and constructing reanalyses of atmospheric composition. Numerous advances have been achieved in data assimilation in the past decades, owing to improved satellite retrievals, better parameterized models, and advanced assimilation techniques (Sandu and Chai 2011; Streets et al. 2013; Bocquet et al. 2015). For example, as shown in Fig. 4, the assimilation of space-based NO_2 data has evolved to increasingly high spatial resolution in recent years.

Data assimilation techniques solve for the statistically optimal solution based on observations and models (Kalnay et al. 2007). Filtering approaches such as the ensemble Kalman filter (EnKF) capture chemical nonlinearities using an ensemble of models and estimate emissions at regional (Tang et al. 2013; Yumimoto et al. 2014; Gaubert et al. 2020; Feng et al. 2020; Dai et al. 2021; van der Graaf et al. 2022) and global (Miyazaki et al. 2012, 2020a; Gaubert et al. 2023) scales. The 4D-Var method utilizes the adjoint of forward models to minimize the model-observation mismatch. Although the development of adjoint models can be complex and running them can be computationally costly, 4D-Var has been successfully implemented for various applications (Elbern et al. 2000; Müller and Stavrakou 2005; Henze et al. 2007). 4D-Var is also used in the Integrated Forecasting System (IFS) of the European Union's Copernicus Atmosphere Monitoring Service (CAMS) (Inness et al. 2015, 2019, 2022).

Simultaneous joint assimilations of multiple species, such as CO/NO_2 (Müller and Stavrakou 2005), HCHO/CHOCHO (Stavrakou et al. 2009; Cao et al. 2018), SO_2/NO_2 (Qu et al. 2019; Wang et al. 2020), and $NO_2/CO/SO_2$ (Miyazaki et al. 2017, 2020a,b), have shown to improve data assimilation results, as they account for the impact of emission changes on the chemical lifetimes of various species. Specifically, assimilating short-lived species can help better characterize the budget of longer-lived gases (e.g., Gaubert et al. 2017; Zheng et al. 2019). To address the increased computational cost of multispecies data assimilation, hybrid approaches combining 4D-Var and mass balance have been recently developed to improve the computational efficiency (Qu et al. 2017, 2019; Y. Chen et al. 2021).

d. Application of machine learning. Machine learning has recently become a popular choice for satellite retrievals due to its higher computational efficiency with respect to traditional retrieval methods. One of the first machine learning applications widely used in data products is the operational IASI NH_3 retrievals based on neural networks (Whitburn et al. 2016; Van Damme et al. 2017). Following that, new data products have been developed for IASI, e.g., the acetone and ethylene retrievals (Franco et al. 2019, 2022) and the CrIS data products (Wells et al. 2022, 2024).

An emerging application of machine learning studies is the estimation of surface concentrations using neural networks and tree-based models for $PM_{2.5}$ (Di et al. 2019; Wei et al. 2020; Pendergrass et al. 2022), O_3 (Sayeed et al. 2021; Betancourt et al. 2022), NO_2

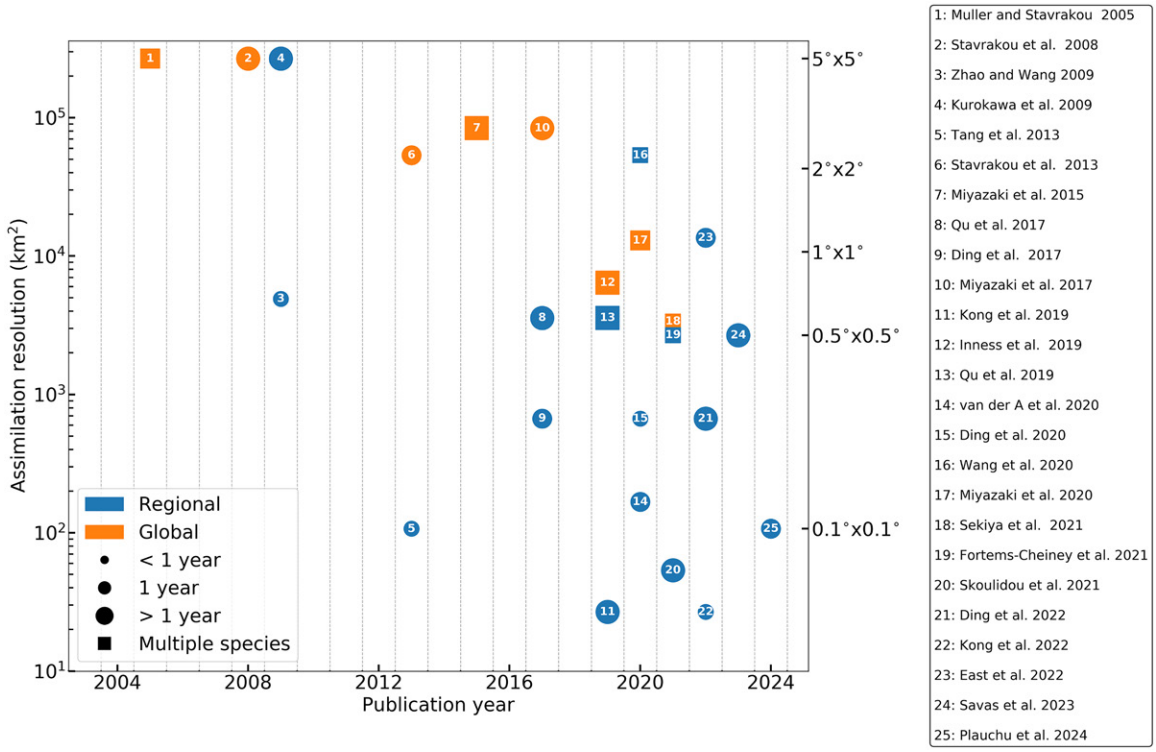

FIG. 4. Evolution of the spatial resolution of space-based NO_2 DA studies over the past two decades. Orange symbols denote global studies, and blue symbols denote regional studies. Circles describe DA systems in which only NO_2 is assimilated. Squares represent multispecies DA studies. The size of the symbol represents the temporal scale.

(Di et al. 2020; Ghahremanloo et al. 2021; Chan et al. 2021), CO (Han et al. 2022; Chen et al. 2024), and CH_4 (Balasus et al. 2023). These studies rely on the fusion of data from multiple sources and show improved skill compared to conventional approaches (Balasus et al. 2023; Oak et al. 2024; Huang et al. 2024). Other research directions include the development of surrogate models or modules in conventional modeling systems with an improved efficiency (Keller and Evans 2019; Kelp et al. 2020, 2022; He et al. 2024b). Using machine learning to understand drivers of air pollution (Zhang et al. 2023; Ma et al. 2023; Wang et al. 2024) and conduct trend analysis (He et al. 2022a; Pendergrass et al. 2022, 2025; Li et al. 2023) are other intriguing directions. The potential of machine learning in the inverse modeling of emissions has also been explored (Huang et al. 2021; He et al. 2022b).

4. Challenges and opportunities in the era of geostationary space observations

Space observations from GEO offer a number of opportunities for improved characterization of air quality and emissions as compared to LEO observations. The higher observation density due to more frequent return times allows for higher precision. It also facilitates cloud clearing, meaning an increased probability of observing a cloud-free scene in a certain location (or adjacent locations) over a certain time period. The continuous observation available from GEO instruments enables the tracking of pollution transport on meso- and synoptic scales. Multiple measurements during the day provide information on the diurnal variations of emissions and chemical evolution. However, there are also important challenges in the retrieval and the interpretation of GEO observations. Next, we elaborate on the opportunities and challenges in retrieval development (section 4a), atmospheric composition modeling (section 4b), data assimilation (section 4c), and machine learning applications for GEO observations (section 4d), and we discuss air quality research for large world regions that are not covered by the planned GEO satellite constellation (section 4e).

a. Retrievals. For GEO observations, not only do the pollutant concentrations change over the day but also the position of the Sun, the surface temperature, the vertical mixing of the atmosphere, and meteorology also change. These parameters are either input variables or impact the a priori vertical profile of the trace gases being retrieved, of which the hourly variations need to be accounted for in retrieval algorithms.

An important aspect is the variation in surface reflectivity for UV–Vis retrievals. Larger reflectivity increases the sensitivity of satellite measurements to trace gases close to the surface, and not considering the diurnal variations in surface reflectivity could lead to artifacts in the retrieved diurnal variation of pollutants. While surface reflectivity information is available from satellite observations, the temporal and spatial resolution may not be sufficient, and uncertainties can be large for individual observations. A similar problem exists for TIR retrievals, where surface radiation emission is strongly dependent on temperature.

A second challenge is the diurnal variation due to vertical mixing, which can change the sensitivity of the satellite measurements to different vertical layers in the atmosphere (Yang et al. 2023a). For UV–Vis retrievals, sensitivity is usually lowest close to the surface, and a shallow boundary layer in the morning reduces sensitivity compared to a fully developed boundary layer in the afternoon. The situation can further be complicated by residual aerosols above the boundary layer. Similar issues are expected from the combination of vertical trace gas distributions and temperature profiles for TIR observations. To account for these effects, atmospheric models used as a priori information in retrievals must reflect the diurnal evolution of the boundary layer, which can be challenging over complex urban areas and terrain.

The viewing geometry from GEO can also present challenges, especially for higher latitudes and at the edges of the field of regard. For UV–Vis observations, large viewing zenith angles can lead to increased scattering in the atmosphere and reduced sensitivity to trace gases near the surface. The effect is further amplified by the presence of aerosols and clouds. Spatial oversampling might have limited use for GEO observations due to the nearly constant ground pixel pattern, as reported in Lange et al. (2024) for the case of GEMS. A possible solution would be to adjust the latitudinal pointing and longitudinal sampling of GEO measurements, but this may complicate the retrievals of aerosol, cloud and gases, and their diurnal variations, which depend on accurate surface reflectance characterization. The pointing of TEMPO has a standard deviation of ~1 pixel due to jitter and other uncertainties, so oversampling can still be useful for TEMPO.

For some trace gases, such as O_3 and NO_2, significant amounts are present in both the troposphere and the stratosphere. This necessitates a stratospheric correction, which, in the case of GEO observations, also needs to account for the diurnal change of the stratospheric amounts. This is particularly relevant for small signals, which are more affected by uncertainties in the stratospheric correction.

Given the challenges outlined above, robust calibration and validation of GEO observations becomes essential to ensure a consistent retrieval quality across different sensors and GEO regions. The calibration and validation efforts for GEO observations will build on the experience from heritage LEO missions (CEOS 2019). These efforts should be supplemented by intensive ground-based and aircraft validation campaigns to evaluate the diurnal patterns measured by the GEO satellites (see, e.g., Kim et al. 2023; Lee et al. 2024; Lange et al. 2024; Ha et al. 2024). LEO air quality missions will serve as a traveling standard for the intercomparability of the different GEO instruments. Further efforts should focus on the development of an harmonized framework for the processing, validation, and publication of all data products from the constellation of GEO composition observations (CEOS 2019).

The availability of multiple measurements per day also provides opportunities for improved retrieval techniques. For example, the nearly simultaneous observation of contiguous

scenes facilitates cloud slicing, where differences in column amounts above optically thick clouds are used to provide information on vertical distribution (Marais et al. 2021). Imagers and spectrometers on GEO platforms, combined with LEO missions, will deliver measurements of multiple chemical species over emission hotspots across a broad spectral range. This expanded coverage has the potential to enable the retrieval of new information and deepen our understanding of emission activities.

b. Modeling. GEO composition observations will be useful for the evaluation of high-resolution regional and local chemical transport models and specifically to compare calculated diurnal variations with the hourly data provided by the retrievals. The measured variations in column concentrations may be very different from the time evolution of surface concentrations (e.g., Tang et al. 2021). A full understanding of the observed diurnal variation is not straightforward because, in addition to the time-evolving forcing from solar radiation, it is driven by other factors such as local emissions and boundary layer meteorology (Edwards et al. 2024). One challenge is to improve the representation of small-scale dynamical features in the planetary boundary layer, including the formation of the heat island in urban areas, the development of convective cells and local cloudiness, the impact of topography and buildings on the small-scale flow, and the influence of diurnal varying coastal circulation cells.

Regional chemical–meteorological models at a spatial resolution of typically 1–5 km are used to provide background information on the chemical composition; they are now often complemented by numerical simulations of large eddies in the boundary layer to resolve their impact on the reaction rates and on chemical segregation associated with emission heterogeneity in a complex urban canopy (Wang et al. 2022). Street network models such as the Model of Urban Network of Intersecting Canyons and Highways (MUNICH) model (Kim et al. 2018) provide the distribution of chemically reactive pollutants along street canyons. The success of such approaches depends on the availability of detailed high-resolution (better than 1 km) emission inventories, which are usually not yet available.

Recent efforts have led to the development of global multiscale models with grid refinement capabilities over selected geographical regions. An irregular model grid with a grid refinement capability over the three regions covered by GEMS, TEMPO, and Sentinel-4 has been developed as part of the next-generation community modeling infrastructure, the Multi-Scale Infrastructure for Chemistry and Aerosols (MUSICA; Pfister et al. 2020). Its purpose is to insert high-resolution regional information provided by the GEO satellites in a global modeling framework that accounts for large-scale transport and distant influences on chemical species (Pfister et al. 2020).

c. Data assimilation. There are several challenges related to the assimilation of GEO observations. The efficient assimilation of such dense observations will require high-resolution forecast models and appropriate data assimilation techniques, in addition to a flexible system handling multiple satellite sensors from both GEO and LEO. As summarized below, further innovations are needed to take advantage of GEO satellite observations with data assimilation.

1) Parameter estimation: In tropospheric chemistry, boundary conditions, reaction rates, and emissions often play an important role, whereas the role of initial conditions is limited due to rapid chemical reactions (Sandu and Chai 2011; Goris and Elbern 2013). Dense observations from GEO satellites may allow for detailed parameter estimation beyond a few key chemical species, improved sectoral emissions estimates (Qu et al. 2022a; Gaubert et al. 2023), and speciation information for VOCs and

aerosols. They can also be used to correct for meteorological parameters such as horizontal wind (Liu et al. 2021).

2) Data assimilation methodology: With greater observational coverage and high measurement accuracy, local emission sources could be estimated using computationally efficient approaches such as the mass balance approach (e.g., Cooper et al. 2017; Qu et al. 2017; Qu et al. 2019) or by making use of trajectories to describe the nonlocal relation between emissions and concentrations (e.g., van der A et al. 2024). Nevertheless, flow-dependent background covariance, including covariance among chemical species, is essential to integrate multiple-species information and their spatial distributions. Data assimilation (DA) techniques also need to account for diurnal changes in chemistry, emissions, and measurement characteristics (e.g., Timmermans et al. 2019; Shu et al. 2023). Efficient non-Gaussian methods such as particle filters may also be needed for high-resolution DA (Valmassoi et al. 2023).
3) Plume analysis and emission estimates: The latest GEO and LEO satellite composition observations are able to resolve plumes of urban emissions, major point sources (e.g., van der A et al. 2020), and even individual ships (e.g., Riess et al. 2022). Computationally efficient techniques such as plume fitting (e.g., Fioletov et al. 2017), the flux-divergence technique (e.g., Beirle et al. 2023), or the integrated mass enhancement method (e.g., Varon et al. 2018; He et al. 2024a) have been successful in providing emission estimates for short-lived and long-lived tracers at the instrumental resolution. A major challenge for short-lived compounds like NO_2 is to account for the nonlinear chemistry in plumes, leading to a heterogeneous plume composition and lifetime (Krol et al. 2024), and to determine how these local effects impact global or regional data assimilation systems.
4) Combination of multiple observing systems: LEO composition observations provide constraints on long-range transport (Miyazaki et al. 2022) and reduce model errors in regions constrained by GEO composition observations. Well-validated LEO data can be used to benchmark GEO composition observations, for example, as an anchor for DA bias correction. As the spatial resolution of both forecast models and satellites increases, assimilation of in situ and satellite observations will be another effective approach to improve analysis, especially near the surface. New technical challenges for simultaneous assimilation include appropriate background error covariance at multiple scales and error statistics including representative errors of each measurement (Wang and Wang 2023).

d. Machine learning. For future applications of machine learning in air quality research, the differences between LEO and GEO viewing geometries need to be accounted for. Solar zenith angle and viewing zenith angle could have greater importance when constructing machine learning models for retrieving atmospheric composition from GEO satellites. Diurnal variations in related physical parameters should also be captured by input variables for machine learning models for GEO composition satellites.

Recent applications of machine learning for LEO atmospheric composition satellites have focused on concentration estimation and the development of surrogate models. More efforts are needed in applying machine learning to inverse modeling of emissions. Specifically, further development of explainable machine learning models is necessary to enhance the interpretability and robustness of emission estimates.

Despite the challenges, geostationary atmospheric composition satellites offer opportunities to further advance innovation in future machine learning applications. For example, machine learning is effective in anomaly detection and pattern recognition, both making it well suited for monitoring extreme events (e.g., wildfires and volcano eruptions). Its scalability to the

high temporal and spatial resolution of GEO composition measurements can be critical for real-time decision-making and mitigating the impacts of extreme events.

The generalizability of machine learning is another key strength that enhances data fusion. Recent studies indicate that integrating multisource measurements using machine learning can help reduce discrepancies between different datasets (Balasus et al. 2023; Oak et al. 2024; Huang et al. 2024). Integrating LEO composition measurements can play a critical role in improving the consistency of composition measurements made by different GEO satellites.

e. Atmospheric composition monitoring for other regions of the world. Space-borne instruments in LEO have been vital for addressing data sparsity in large parts of the world, in particular for the African and South American continents and parts of Asia. These regions will continue to rely on LEO instruments, as the planned GEO satellite constellation mainly covers the Northern Hemisphere (Paton-Walsh et al. 2022). The validation of both LEO and GEO observations and the derived products is also rare across the tropics and Southern Hemisphere. Such validation requires routine surface observations and aircraft campaigns to profile the troposphere under a range of representative conditions (Tang et al. 2023).

The Sentinel-4 GEO composition instrument will observe a portion of North Africa, and the IRS on the same platform will provide observations of infrared-absorbing compounds like CO and NH_3. CO observations over Africa will be vital for understanding inefficient combustion sources, including biomass burning for agricultural practices in Africa (Andreae 2019), burning of waste (Wiedinmyer et al. 2014), and from other inefficient combustion practices (Marais and Wiedinmyer 2016; Bockarie et al. 2020). High-frequency NH_3 observations are well timed to coincide with agricultural intensification that includes the use of synthetic nitrogen fertilizer and intensive livestock farming (Hickman et al. 2021). A demonstration of the utility of GEO observations of NH_3 and CO for informing diurnal changes in abundances, precursor emissions, and pollution transport patterns over Africa would aid in advocating for dedicated GEO instruments over Africa and South America. However, the long delay between mission concept and launch means missing out on advancing understanding in regions of the world during a period of unprecedented population growth and land-use changes. An advisory committee comprising researchers, academics, and satellite instrument developers has been formed to propose GEO missions over Africa and South America, but a greater representation of researchers from these regions is needed to inform the development of a fit-for-purpose mission (Marais and Chance 2015).

5. Conclusions and recommendations

The implementation of GEO satellites for atmospheric composition monitoring opens new perspectives for air quality research. The first two GEO composition satellites over Asia and North America have demonstrated the measurement of diurnal variation of chemical species, thereby providing unprecedented information on the diel evolution of emissions, photochemical processes, and the effects of atmospheric dynamics over large regions. However, the development of retrievals and the validation of these GEO satellite composition data is still ongoing, as there is still room for improvement. Furthermore, the European component of the GEO constellation in Sentinel-4 is expected to be launched in 2025. The exploitation of measurements conducted by GEO satellites presents new challenges and several priority tasks can therefore be highlighted for future research.

- Retrieval algorithms need to be carefully adapted to the GEO composition observations. Specifically, the diurnal variations of various parameters used in the retrieval, such as surface reflectivity and vertical mixing, need to be resolved. Additionally, the viewing

geometry can present difficulties due to the large zenith angles of GEO instruments compared to nadir-viewing satellites; hence, correcting for these effects at the edges of the field of regard is necessary.
- The hourly temporal resolution of GEO observations gives crucial information on diurnal profiles of emissions of atmospheric pollutants. In order to leverage this aspect in emission inversion studies and reduce the delay in the delivery of emission inventories, temporal profiles for different sectors in emission inventories need to be provided.
- Global and regional models should be adapted to be more compatible with the GEO atmospheric composition satellites. Continuous model development, especially regarding the fine-scale chemical processes, is essential for retrievals, air quality forecasting, and data assimilation in the era of GEO satellites for atmospheric composition monitoring.
- Data assimilation methods need to be adapted to the geostationary case. Specifically, more computationally efficient methods should be explored in order to optimally process the high data volume. The coexistence of LEO and GEO measurements in the same area opens possibilities to assimilate both datasets simultaneously, along with ground-based and aircraft data. Deriving emissions from point sources from plume estimation methods also provides a promising avenue, considering the higher temporal resolution of observations.
- The computational efficiency and generalizability of machine learning make it a valuable area for further exploration. In addition to recent applications of machine learning in retrieval algorithm development and surface concentration estimation, greater efforts should be directed toward inverse modeling of emissions and the development of explainable models.

Finally, it is crucial to keep improving the accessibility of satellite measurements to agencies in charge of air quality management, especially for regions lacking the capability to establish observation networks. Future GEO satellites should provide data over Africa, South America, southern Asia, Australia, New Zealand, and other regions not covered by the current observing capabilities.

Acknowledgments. This research was supported by the International Space Science Institute (ISSI) in Bern and Beijing, through ISSI/ISSI-Beijing International Team project 489 (Use of Geostationary Satellites to Improve Air Quality Characterization and Forecasts). This work is partially supported by a NASA Early Career Faculty Grant (80NSSC21K1808). A portion of this research was carried out at the Jet Propulsion Laboratory, California Institute of Technology, under a contract with the National Aeronautics and Space Administration (80NM0018D0004). The NSF National Center for Atmospheric Research is sponsored by the National Science Foundation (NSF). The views expressed are those of authors and do not necessarily reflect any position of NOAA or the Department of Commerce.

Data availability statement. The GEMS NO_2 tropospheric column density data are publicly available on request from the National Institute of Environmental Research (NIER) Environmental Satellite Center (ESC) (https://nesc.nier.go.kr/en/html/datasvc/data.do?pageIndex=1&outputInnb=64&atrb=NO2_Trop, last access: 3 August 2024). The TEMPO NO_2 tropospheric columns are openly available from the NASA Earthdata Atmospheric Science Data Center (https://asdc.larc.nasa.gov/project/TEMPO/TEMPO_NO2_L2_V01 with https://doi.org/10.5067/IS-40e/TEMPO/NO2_L2.001, last access: 3 August 2024). The TROPOMI monthly mean NO_2 tropospheric columns are available from the KNMI Tropospheric Emission Monitoring Internet Service (https://www.temis.nl/airpollution/no2col/no2month_tropomi.php, last access: 3 August 2024).

References

Alvarado, L. M. A., A. Richter, M. Vrekoussis, A. Hilboll, A. B. K. Hedegaard, O. Schneising, and J. P. Burrows, 2020: Unexpected long-range transport of glyoxal and formaldehyde observed from the Copernicus Sentinel-5 Precursor satellite during the 2018 Canadian wildfires. *Atmos. Chem. Phys.*, **20**, 2057–2072, https://doi.org/10.5194/acp-20-2057-2020.

Andreae, M. O., 2019: Emission of trace gases and aerosols from biomass burning—An updated assessment. *Atmos. Chem. Phys.*, **19**, 8523–8546, https://doi.org/10.5194/acp-19-8523-2019.

Arellano, A. F., P. S. Kasibhatla, L. Giglio, G. R. van der Werf, and J. T. Randerson, 2004: Top-down estimates of global CO sources using MOPITT measurements. *Geophys. Res. Lett.*, **31**, L01104, https://doi.org/10.1029/2003GL018609.

Baek, K., J. H. Kim, J. Bak, D. P. Haffner, M. Kang, and H. Hong, 2023: Evaluation of total ozone measurements from Geostationary Environmental Monitoring Spectrometer (GEMS). *Atmos. Meas. Tech.*, **16**, 5461–5478, https://doi.org/10.5194/amt-16-5461-2023.

Bak, J., X. Liu, K. Yang, G. Gonzalez Abad, E. O'Sullivan, K. Chance, and C.-H. Kim, 2024: An improved OMI ozone profile research product version 2.0 with collection 4 L1b data and algorithm updates. *Atmos. Meas. Tech.*, **17**, 1891–1911, https://doi.org/10.5194/amt-17-1891-2024.

Balasus, N., and Coauthors, 2023: A blended TROPOMI+GOSAT satellite data product for atmospheric methane using machine learning to correct retrieval biases. *Atmos. Meas. Tech.*, **16**, 3787–3807, https://doi.org/10.5194/amt-16-3787-2023.

Bauwens, M., and Coauthors, 2016: Nine years of global hydrocarbon emissions based on source inversion of OMI formaldehyde observations. *Atmos. Chem. Phys.*, **16**, 10133–10158, https://doi.org/10.5194/acp-16-10133-2016.

——, and Coauthors, 2020: Impact of coronavirus outbreak on NO_2 pollution assessed using TROPOMI and OMI observations. *Geophys. Res. Lett.*, **47**, e2020GL087978, https://doi.org/10.1029/2020GL087978.

Beirle, S., K. F. Boersma, U. Platt, M. G. Lawrence, and T. Wagner, 2011: Megacity emissions and lifetimes of nitrogen oxides probed from space. *Science*, **333**, 1737–1739, https://doi.org/10.1126/science.1207824.

——, C. Borger, A. Jost, and T. Wagner, 2023: Improved catalog of NO_x point source emissions (version 2). *Earth Syst. Sci. Data*, **15**, 3051–3073, https://doi.org/10.5194/essd-15-3051-2023.

Betancourt, C., T. T. Stomberg, A.-K. Edrich, A. Patnala, M. G. Schultz, R. Roscher, J. Kowalski, and S. Stadtler, 2022: Global, high-resolution mapping of tropospheric ozone—Explainable machine learning and impact of uncertainties. *Geosci. Model Dev.*, **15**, 4331–4354, https://doi.org/10.5194/gmd-15-4331-2022.

Bhartia, P. K., R. D. McPeters, L. E. Flynn, S. Taylor, N. A. Kramarova, S. Frith, B. Fisher, and M. DeLand, 2013: Solar Backscatter UV (SBUV) total ozone and profile algorithm. *Atmos. Meas. Tech.*, **6**, 2533–2548, https://doi.org/10.5194/amt-6-2533-2013.

Bockarie, A. S., E. A. Marais, and A. R. MacKenzie, 2020: Air pollution and climate forcing of the charcoal industry in Africa. *Environ. Sci. Technol.*, **54**, 13429–13438, https://doi.org/10.1021/acs.est.0c03754.

Bocquet, M., and Coauthors, 2015: Data assimilation in atmospheric chemistry models: Current status and future prospects for coupled chemistry meteorology models. *Atmos. Chem. Phys.*, **15**, 5325–5358, https://doi.org/10.5194/acp-15-5325-2015.

Bovensmann, H., J. P. Burrows, M. Buchwitz, J. Frerick, S. Noël, V. V. Rozanov, K. V. Chance, and A. P. H. Goede, 1999: SCIAMACHY: Mission objectives and measurement modes. *J. Atmos. Sci.*, **56**, 127–150, https://doi.org/10.1175/1520-0469(1999)056<0127:SMOAMM>2.0.CO;2.

Brasseur, G., and C. Granier, 2020: Use of geostationary satellites to improve air quality characterization and forecasts. https://www.issibern.ch/scientific-opportunities/international-teams/.

Buchholz, R. R., and Coauthors, 2021: Air pollution trends measured from Terra: CO and AOD over industrial fire-prone and background regions. *Remote Sens. Environ.*, **256**, 112275–112275, https://doi.org/10.1016/j.rse.2020.112275.

Burrows, J. P., and Coauthors, 1999: The Global Ozone Monitoring Experiment (GOME): Mission concept and first scientific results. *J. Atmos. Sci.*, **56**, 151–175, https://doi.org/10.1175/1520-0469(1999)056<0151:TGOMEG>2.0.CO;2.

Cao, H., and Coauthors, 2018: Adjoint inversion of Chinese non-methane volatile organic compound emissions using space-based observations of formaldehyde and glyoxal. *Atmos. Chem. Phys.*, **18**, 15017–15046, https://doi.org/10.5194/acp-18-15017-2018.

Carmichael, G. R., A. Sandu, T. Chai, D. N. Daescu, E. M. Constantinescu, and Y. Tang, 2008: Predicting air quality: Improvements through advanced methods to integrate models and measurements. *J. Comput. Phys.*, **227**, 3540–3571, https://doi.org/10.1016/j.jcp.2007.02.024.

Carr, J., X. Liu, B. Baker, and K. Chance, 2017: Observing nightlights from space with TEMPO. *Int. J. Sustainable Light.*, **19**, 26–35, https://doi.org/10.26607/ijsl.v19i1.64.

CEOS, 2019: Geostationary satellite constellation for observing global air quality: Geophysical validation needs. CEOS Atmospheric Composition Virtual Constellation and the CEOS Working Group on Calibration and Validation Tech. Rep., 47 pp., https://ceos.org/observations/documents/GEO_AQ_Constellation_Geophysical_Validation_Needs_1.1_2Oct2019.pdf.

Chan, K. L., E. Khorsandi, S. Liu, F. Baier, and P. Valks, 2021: Estimation of surface NO_2 concentrations over Germany from TROPOMI satellite observations using a machine learning method. *Remote Sens.*, **13**, 969, https://doi.org/10.3390/rs13050969.

Chen, B., J. Hu, and Y. Wang, 2024: Synergistic observation of FY-4A&4B to estimate CO concentration in China: Combining interpretable machine learning to reveal the influencing mechanisms of CO variations. *npj Climate Atmos. Sci.*, **7**, 9, https://doi.org/10.1038/s41612-023-00559-0.

Chen, X., and Coauthors, 2021: First retrieval of absorbing aerosol height over dark target using TROPOMI oxygen B band: Algorithm development and application for surface particulate matter estimates. *Remote Sens. Environ.*, **265**, 112674, https://doi.org/10.1016/j.rse.2021.112674.

Chen, Y., and Coauthors, 2021: High-resolution hybrid inversion of IASI ammonia columns to constrain US ammonia emissions using the CMAQ adjoint model. *Atmos. Chem. Phys.*, **21**, 2067–2082, https://doi.org/10.5194/acp-21-2067-2021.

Cho, Y., and Coauthors, 2024: First atmospheric aerosol-monitoring results from Geostationary Environment Monitoring Spectrometer (GEMS) over Asia. *Atmos. Meas. Tech.*, **17**, 4369–4390, https://doi.org/10.5194/amt-17-4369-2024.

Clarisse, L., Y. R'Honi, P.-F. Coheur, D. Hurtmans, and C. Clerbaux, 2011: Thermal infrared nadir observations of 24 atmospheric gases. *Geophys. Res. Lett.*, **38**, L10802, https://doi.org/10.1029/2011GL047271.

——, M. Van Damme, C. Clerbaux, and P.-F. Coheur, 2019: Tracking down global NH_3 point sources with wind-adjusted superresolution. *Atmos. Meas. Tech.*, **12**, 5457–5473, https://doi.org/10.5194/amt-12-5457-2019.

——, ——, D. Hurtmans, B. Franco, C. Clerbaux, and P.-F. Coheur, 2021: The diel cycle of NH_3 observed from the FY-4A Geostationary Interferometric Infrared Sounder (GIIRS). *Geophys. Res. Lett.*, **48**, e2021GL093010, https://doi.org/10.1029/2021GL093010.

——, and Coauthors, 2023: The IASI NH_3 version 4 product: Averaging kernels and improved consistency. *Atmos. Meas. Tech.*, **16**, 5009–5028, https://doi.org/10.5194/amt-16-5009-2023.

Clerbaux, C., and Coauthors, 2009: Monitoring of atmospheric composition using the thermal infrared IASI/MetOp sounder. *Atmos. Chem. Phys.*, **9**, 6041–6054, https://doi.org/10.5194/acp-9-6041-2009.

——, and Coauthors, 2013: New directions: Infrared remote sensing of the troposphere from satellite: Less, but better. *Atmos. Environ.*, **72**, 24–26, https://doi.org/10.1016/j.atmosenv.2013.01.057.

Cohen, A. J., and Coauthors, 2017: Estimates and 25-year trends of the global burden of disease attributable to ambient air pollution: An analysis of data

from the global burden of diseases study 2015. *Lancet*, **389**, 1907–1918, https://doi.org/10.1016/S0140-6736(17)30505-6.

Cooper, M., R. V. Martin, A. Padmanabhan, and D. K. Henze, 2017: Comparing mass balance and adjoint methods for inverse modeling of nitrogen dioxide columns for global nitrogen oxide emissions. *J. Geophys. Res. Atmos.*, **122**, 4718–4734, https://doi.org/10.1002/2016JD025985.

Coopmann, O., N. Fourrié, P. Chambon, J. Vidot, P. Brousseau, M. Martet, and C. Birman, 2023: Preparing the assimilation of the future MTG-IRS sounder into the mesoscale numerical weather prediction AROME model. *Quart. J. Roy. Meteor. Soc.*, **149**, 3110–3134, https://doi.org/10.1002/qj.4548.

Crevoisier, C., and Coauthors, 2014: Towards IASI-New Generation (IASI-NG): Impact of improved spectral resolution and radiometric noise on the retrieval of thermodynamic, chemistry and climate variables. *Atmos. Meas. Tech.*, **7**, 4367–4385, https://doi.org/10.5194/amt-7-4367-2014.

Crippa, M., and Coauthors, 2023a: GHG emissions of all world countries. Publications Office of the European Union Tech. Rep. JRC134504, 268 pp., https://doi.org/10.2760/953322.

——, and Coauthors, 2023b: The HTAP_v3 emission mosaic: Merging regional and global monthly emissions (2000–2018) to support air quality modelling and policies. *Earth Syst. Sci. Data*, **15**, 2667–2694, https://doi.org/10.5194/essd-15-2667-2023.

——, and Coauthors, 2024: EDGAR v8.1 global air pollutant emissions. European Commission, Joint Research Centre, accessed 13 June 2023, https://data.europa.eu/89h/a3af16e4-21ac-420a-b98c-b78a9b7723be.

Dai, T., Y. Cheng, D. Goto, Y. Li, X. Tang, G. Shi, and T. Nakajima, 2021: Revealing the sulfur dioxide emission reductions in China by assimilating surface observations in WRF-Chem. *Atmos. Chem. Phys.*, **21**, 4357–4379, https://doi.org/10.5194/acp-21-4357-2021.

Damme, M. V., L. Clarisse, T. Stavrakou, R. W. Kruit, L. Sellekaerts, C. Viatte, C. Clerbaux, and P.-F. Coheur, 2022: On the weekly cycle of atmospheric ammonia over European agricultural hotspots. *Sci. Rep.*, **12**, 12327, https://doi.org/10.1038/s41598-022-15836-w.

Dechezleprêtre, A., N. Rivers, and B. Stadler, 2019: The economic cost of air pollution: Evidence from Europe. OECD Economics Department Working Paper 1584, 63 pp., https://www.oecd.org/en/publications/the-economic-cost-of-air-pollution-evidence-from-europe_56119490-en.html.

Di, Q., and Coauthors, 2019: An ensemble-based model of $PM_{2.5}$ concentration across the contiguous United States with high spatiotemporal resolution. *Environ. Int.*, **130**, 104909, https://doi.org/10.1016/j.envint.2019.104909.

——, and Coauthors, 2020: Assessing NO_2 concentration and model uncertainty with high spatiotemporal resolution across the contiguous United States using ensemble model averaging. *Environ. Sci. Technol.*, **54**, 1372–1384, https://doi.org/10.1021/acs.est.9b03358.

Douros, J., and Coauthors, 2023: Comparing Sentinel-5P TROPOMI NO_2 column observations with the CAMS regional air quality ensemble. *Geosci. Model Dev.*, **16**, 509–534, https://doi.org/10.5194/gmd-16-509-2023.

Drummond, J. R., and G. S. Mand, 1996: The Measurements of Pollution in the Troposphere (MOPITT) instrument: Overall performance and calibration requirements. *J. Atmos. Oceanic Technol.*, **13**, 314–320, https://doi.org/10.1175/1520-0426(1996)013<0314:TMOPIT>2.0.CO;2.

——, Z. Vaziri Zanjani, F. Nichitiu, and J. Zou, 2022: A 20-year review of the performance and operation of the MOPITT instrument. *Adv. Space Res.*, **70**, 3078–3091, https://doi.org/10.1016/j.asr.2022.09.010.

Duncan, B. N., L. N. Lamsal, A. M. Thompson, Y. Yoshida, Z. Lu, D. G. Streets, M. M. Hurwitz, and K. E. Pickering, 2016: A space-based, high-resolution view of notable changes in urban NO_x pollution around the world (2005–2014). *J. Geophys. Res. Atmos.*, **121**, 976–996, https://doi.org/10.1002/2015JD024121.

Edwards, D. P., and Coauthors, 2024: Quantifying the diurnal variation in atmospheric NO_2 from Geostationary Environment Monitoring Spectrometer (GEMS) observations. *Atmos. Chem. Phys.*, **24**, 8943–8961, https://doi.org/10.5194/acp-24-8943-2024.

Elbern, H., H. Schmidt, O. Talagrand, and A. Ebel, 2000: 4D-variational data assimilation with an adjoint air quality model for emission analysis. *Environ. Modell. Software*, **15**, 539–548, https://doi.org/10.1016/S1364-8152(00)00049-9.

Elguindi, N., and Coauthors, 2020: Intercomparison of magnitudes and trends in anthropogenic surface emissions from bottom-up inventories top-down estimates and emission scenarios. *Earth's Future*, **8**, e2020EF001520, https://doi.org/10.1029/2020ef001520.

Environment and Climate Change Canada, 2019: Canada's air pollutant emissions inventory report. Environment and Climate Change Canada, https://publications.gc.ca/site/eng/9.869731/publication.html.

Eskes, H., and Coauthors, 2024: Technical note: Evaluation of the Copernicus Atmosphere Monitoring Service Cy48R1 upgrade of June 2023. *Atmos. Chem. Phys.*, **24**, 9475–9514, https://doi.org/10.5194/acp-24-9475-2024.

Eskes, H. J., and K. F. Boersma, 2003: Averaging kernels for DOAS total-column satellite retrievals. *Atmos. Chem. Phys.*, **3**, 1285–1291, https://doi.org/10.5194/acp-3-1285-2003.

European Environment Agency, 2023: EMEP/EEA air pollutant emission inventory guidebook 2023: Technical guidance to prepare national emission inventories. European Environment Agency, 30 pp., https://doi.org/10.2800/795737.

Feng, S., F. Jiang, Z. Wu, H. Wang, W. Ju, and H. Wang, 2020: CO emissions inferred from surface CO observations over China in December 2013 and 2017. *J. Geophys. Res. Atmos.*, **125**, e2019JD031808, https://doi.org/10.1029/2019JD031808.

Fioletov, V., and Coauthors, 2017: Multi-source SO_2 emission retrievals and consistency of satellite and surface measurements with reported emissions. *Atmos. Chem. Phys.*, **17**, 12 597–12 616, https://doi.org/10.5194/acp-17-12597-2017.

——, C. A. McLinden, D. Griffin, N. Theys, D. G. Loyola, P. Hedelt, N. A. Krotkov, and C. Li, 2020: Anthropogenic and volcanic point source SO_2 emissions derived from TROPOMI on board Sentinel-5 Precursor: First results. *Atmos. Chem. Phys.*, **20**, 5591–5607, https://doi.org/10.5194/acp-20-5591-2020.

Fioletov, V. E., C. A. McLinden, N. Krotkov, and C. Li, 2015: Lifetimes and emissions of SO_2 from point sources estimated from OMI. *Geophys. Res. Lett.*, **42**, 1969–1976, https://doi.org/10.1002/2015GL063148.

Fortems-Cheiney, A., and Coauthors, 2021: Variational regional inverse modeling of reactive species emissions with PYVAR-CHIMERE-v2019. *Geosci. Model Dev.*, **14**, 2939–2957, https://doi.org/10.5194/gmd-14-2939-2021.

Franco, B., and Coauthors, 2018: A general framework for global retrievals of trace gases from IASI: Application to methanol, formic acid, and PAN. *J. Geophys. Res. Atmos.*, **123**, 13 963–13 984, https://doi.org/10.1029/2018JD029633.

——, and Coauthors, 2019: Acetone atmospheric distribution retrieved from space. *Geophys. Res. Lett.*, **46**, 2884–2893, https://doi.org/10.1029/2019GL082052.

——, L. Clarisse, M. V. Damme, J. Hadji-Lazaro, C. Clerbaux, and P.-F. Coheur, 2022: Ethylene industrial emitters seen from space. *Nat. Commun.*, **13**, 6452, https://doi.org/10.1038/s41467-022-34098-8.

Frederick, S. E., R. P. Cebula, and D. F. Heath, 1986: Instrument characterization for the detection of long-term changes in stratospheric ozone: An analysis of the SBUY/2 radiometer. *J. Atmos. Oceanic Technol.*, **3**, 472–480, https://doi.org/10.1175/1520-0426(1986)003<0472:ICFTDO>2.0.CO;2.

Fu, D., D. B. Millet, K. C. Wells, V. H. Payne, S. Yu, A. Guenther, and A. Eldering, 2019: Direct retrieval of isoprene from satellite-based infrared measurements. *Nat. Commun.*, **10**, 3811, https://doi.org/10.1038/s41467-019-11835-0.

Fu, T., and Coauthors, 2007: Space-based formaldehyde measurements as constraints on volatile organic compound emissions in East and South Asia and implications for ozone. *J. Geophys. Res.*, **112**, D06312, https://doi.org/10.1029/2006JD007853.

Gaubert, B., and Coauthors, 2017: Chemical feedback from decreasing carbon monoxide emissions. *Geophys. Res. Lett.*, **44**, 9985–9995, https://doi.org/10.1002/2017GL074987.

——, and Coauthors, 2020: Correcting model biases of CO in East Asia: Impact on oxidant distributions during KORUS-AQ. *Atmos. Chem. Phys.*, **20**, 14 617–14 647, https://doi.org/10.5194/acp-20-14617-2020.

——, and Coauthors, 2023: Global scale inversions from MOPITT CO and MODIS AOD. *Remote Sens.*, **15**, 4813, https://doi.org/10.3390/rs15194813.

Ghahremanloo, M., Y. Lops, Y. Choi, and B. Yeganeh, 2021: Deep learning estimation of daily ground-level NO_2 concentrations from remote sensing data. *J. Geophys. Res. Atmos.*, **126**, e2021JD034925, https://doi.org/10.1029/2021JD034925.

Gkatzelis, G. I., and Coauthors, 2021: The global impacts of COVID-19 lockdowns on urban air pollution. *Elementa*, **9**, 00176, https://doi.org/10.1525/elementa.2021.00176.

Goris, N., and H. Elbern, 2013: Singular vector decomposition for sensitivity analyses of tropospheric chemical scenarios. *Atmos. Chem. Phys.*, **13**, 5063–5087, https://doi.org/10.5194/acp-13-5063-2013.

Government of Canada, 2018: Government of Canada's greenhouse gas emissions inventory. Treasury Board of Canada Secretariat, https://publications.gc.ca/site/eng/9.849459/publication.html.

Granier, C., C. Liousse, B. McDonald, and P. Middleton, 2023: Anthropogenic emissions inventories of air pollutants. *Handbook of Air Quality and Climate Change*, Springer Nature Singapore, 3–52, https://doi.org/10.1007/978-981-15-2760-9_5.

Guanter, L., and Coauthors, 2021: The TROPOSIF global sun-induced fluorescence dataset from the Sentinel-5P TROPOMI mission. *Earth Syst. Sci. Data*, **13**, 5423–5440, https://doi.org/10.5194/essd-13-5423-2021.

Guevara, M., and Coauthors, 2021: Copernicus Atmosphere Monitoring Service TEMPOral profiles (CAMS-TEMPO): Global and European emission temporal profile maps for atmospheric chemistry modelling. *Earth Syst. Sci. Data*, **13**, 367–404, https://doi.org/10.5194/essd-13-367-2021.

Ha, E. S., and Coauthors, 2024: First evaluation of the GEMS glyoxal products against TROPOMI and ground-based measurements. *EGUsphere*, **17**, 6369–6384, https://doi.org/10.5194/amt-17-6369-2024.

Han, S., W. Kundhikanjana, P. Towashiraporn, and D. Stratoulias, 2022: Interpolation-based fusion of Sentinel-5P, SRTM, and regulatory-grade ground stations data for producing spatially continuous maps of $PM_{2.5}$ concentrations nationwide over Thailand. *Atmosphere*, **13**, 161, https://doi.org/10.3390/atmos13020161.

Han, Y., and Coauthors, 2013: Suomi NPP CrIS measurements, sensor data record algorithm, calibration and validation activities, and record data quality. *J. Geophys. Res. Atmos.*, **118**, 12 734–12 748, https://doi.org/10.1002/2013JD020344.

He, T.-L., and Coauthors, 2022a: Deep learning to evaluate US NO_x emissions using surface ozone predictions. *J. Geophys. Res. Atmos.*, **127**, e2021JD03597, https://doi.org/10.1029/2021JD035597.

——, and Coauthors, 2022b: Inverse modelling of Chinese NO_x emissions using deep learning: Integrating in situ observations with a satellite-based chemical reanalysis. *Atmos. Chem. Phys.*, **22**, 14 059–14 074, https://doi.org/10.5194/acp-22-14059-2022.

——, R. J. Boyd, D. J. Varon, and A. J. Turner, 2024a: Increased methane emissions from oil and gas following the Soviet Union's collapse. *Proc. Natl. Acad. Sci. USA*, **121**, e2314600121, https://doi.org/10.1073/pnas.2314600121.

——, N. Dadheech, T. Thompson, and A. Turner, 2024b: FootNet v1.0: Development of a machine learning emulator of atmospheric transport. EarthArXiv, https://doi.org/10.31223/x5197g.

Heath, D. F., A. J. Krueger, H. A. Roeder, and B. D. Henderson, 1975: The Solar Backscatter Ultraviolet and Total Ozone Mapping Spectrometer (SBUV/TOMS) for NIMBUS G. *Opt. Eng.*, **14**, 144 323, https://doi.org/10.1117/12.7971839.

Hedelius, J. K., and Coauthors, 2021: Regional and urban column CO trends and anomalies as observed by MOPITT over 16 years. *J. Geophys. Res. Atmos.*, **126**, e2020JD033967, https://doi.org/10.1029/2020JD033967.

Henze, D. K., A. Hakami, and J. H. Seinfeld, 2007: Development of the adjoint of GEOS-Chem. *Atmos. Chem. Phys.*, **7**, 2413–2433, https://doi.org/10.5194/acp-7-2413-2007.

Heue, K.-P., D. Loyola, F. Romahn, W. Zimmer, S. Chabrillat, Q. Errera, J. Ziemke, and N. Kramarova, 2022: Tropospheric ozone retrieval by a combination of TROPOMI/S5P measurements with BASCOE assimilated data. *Atmos. Meas. Tech.*, **15**, 5563–5579, https://doi.org/10.5194/amt-15-5563-2022.

Hickman, J. E., and Coauthors, 2021: Changes in biomass burning wetland extent or agriculture drive atmospheric NH_3 trends in select African regions. *Atmos. Chem. Phys.*, **21**, 16 277–16 291, https://doi.org/10.5194/acp-21-16277-2021.

Huang, L., and Coauthors, 2021: Exploring deep learning for air pollutant emission estimation. *Geosci. Model Dev.*, **14**, 4641–4654, https://doi.org/10.5194/gmd-14-4641-2021.

Huang, X., Z. Deng, F. Jiang, M. Zhou, X. Lin, Z. Liu, and M. Peng, 2024: Improved consistency of satellite XCO_2 retrievals based on machine learning. *Geophys. Res. Lett.*, **51**, e2023GL107536, https://doi.org/10.1029/2023GL107536.

Hyman, D. M., and M. J. Pavolonis, 2020: Probabilistic retrieval of volcanic SO_2 layer height and partial column density using the Cross-track Infrared Sounder (CrIS). *Atmos. Meas. Tech.*, **13**, 5891–5921, https://doi.org/10.5194/amt-13-5891-2020.

Inness, A., and Coauthors, 2015: Data assimilation of satellite-retrieved ozone carbon monoxide and nitrogen dioxide with ECMWF's Composition-IFS. *Atmos. Chem. Phys.*, **15**, 5275–5303, https://doi.org/10.5194/acp-15-5275-2015.

——, and Coauthors, 2019: The CAMS reanalysis of atmospheric composition. *Atmos. Chem. Phys.*, **19**, 3515–3556, https://doi.org/10.5194/acp-19-3515-2019.

——, and Coauthors, 2022: Assimilation of S5P/TROPOMI carbon monoxide data with the global CAMS near-real-time system. *Atmos. Chem. Phys.*, **22**, 14 355–14 376, https://doi.org/10.5194/acp-22-14355-2022.

Jiang, Z., and Coauthors, 2018: Unexpected slowdown of US pollutant emission reduction in the past decade. *Proc. Natl. Acad. Sci. USA*, **115**, 5099–5104, https://doi.org/10.1073/pnas.1801191115.

——, and Coauthors, 2022: Decadal variabilities in tropospheric nitrogen oxides over United States, Europe, and China. *J. Geophys. Res. Atmos.*, **127**, e2021JD035872, https://doi.org/10.1029/2021JD035872.

Kalnay, E., H. Li, T. Miyoshi, S.-C. Yang, and J. Ballabrera-Poy, 2007: 4-D-Var or ensemble Kalman filter? *Tellus*, **59A**, 758, https://doi.org/10.1111/j.1600-0870.2007.00261.x.

Keita, S., and Coauthors, 2021: African anthropogenic emissions inventory for gases and particles from 1990 to 2015. *Earth Syst. Sci. Data*, **13**, 3691–3705, https://doi.org/10.5194/essd-13-3691-2021.

Keller, C. A., and M. J. Evans, 2019: Application of random forest regression to the calculation of gas-phase chemistry within the GEOS-Chem chemistry model v10. *Geosci. Model Dev.*, **12**, 1209–1225, https://doi.org/10.5194/gmd-12-1209-2019.

Kelp, M. M., D. J. Jacob, J. N. Kutz, J. D. Marshall, and C. W. Tessum, 2020: Toward stable, general machine-learned models of the atmospheric chemical system. *J. Geophys. Res. Atmos.*, **125**, e2020JD032759, https://doi.org/10.1029/2020JD032759.

——, ——, H. Lin, and M. P. Sulprizio, 2022: An online-learned neural network chemical solver for stable long-term global simulations of atmospheric chemistry. *J. Adv. Model. Earth Syst.*, **14**, e2021MS002926, https://doi.org/10.1029/2021MS002926.

Kim, J., and Coauthors, 2020: New era of air quality monitoring from space: Geostationary Environment Monitoring Spectrometer (GEMS). *Bull. Amer. Meteor. Soc.*, **101**, E1–E22, https://doi.org/10.1175/BAMS-D-18-0013.1.

Kim, S., and Coauthors, 2023: First-time comparison between NO_2 vertical columns from Geostationary Environmental Monitoring Spectrometer (GEMS) and Pandora measurements. *Atmos. Meas. Tech.*, **16**, 3959–3972, https://doi.org/10.5194/amt-16-3959-2023.

Kim, Y., Y. Wu, C. Seigneur, and Y. Roustan, 2018: Multi-scale modeling of urban air pollution: Development and application of a Street-in-Grid model (v1.0) by coupling MUNICH (v1.0) and Polair3D (v1.8.1). *Geosci. Model Dev.*, **11**, 611–629, https://doi.org/10.5194/gmd-11-611-2018.

Klimont, Z., K. Kupiainen, C. Heyes, P. Purohit, J. Cofala, P. Rafaj, J. Borken-Kleefeld, and W. Schöpp, 2017: Global anthropogenic emissions of particulate matter including black carbon. *Atmos. Chem. Phys.*, **17**, 8681–8723, https://doi.org/10.5194/acp-17-8681-2017.

Krol, M., B. van Stratum, I. Anglou, and K. F. Boersma, 2024: Evaluating NO_x stack plume emissions using a high-resolution atmospheric chemistry model and satellite-derived NO_2 columns. *Atmos. Chem. Phys.*, **24**, 8243–8262, https://doi.org/10.5194/acp-24-8243-2024.

Kuenen, J., S. Dellaert, A. Visschedijk, J.-P. Jalkanen, I. Super, and H. Denier van der Gon, 2021: Copernicus Atmosphere Monitoring Service regional emissions version 5.1 business-as-usual 2020 (CAMS-REG-v5.1 BAU 2020). Copernicus Atmosphere Monitoring Service, eCCAD, accessed 13 June 2023, https://doi.org/10.24380/eptm-kn40.

Kurokawa, J., and T. Ohara, 2020: Long-term historical trends in air pollutant emissions in Asia: Regional Emission inventory in ASia (REAS) version 3. *Atmos. Chem. Phys.*, **20**, 12 761–12 793, https://doi.org/10.5194/acp-20-12761-2020.

Kurokawa, J.-i., K. Yumimoto, I. Uno, and T. Ohara, 2009: Adjoint inverse modeling of NO_x emissions over eastern China using satellite observations of NO_2 vertical column densities. *Atmos. Environ.*, **43**, 1878–1887, https://doi.org/10.1016/j.atmosenv.2008.12.030.

Lahoz, W. A., and P. Schneider, 2014: Data assimilation: Making sense of Earth Observation. *Front. Environ. Sci.*, **2**, 16, https://doi.org/10.3389/fenvs.2014.00016.

Lambrigtsen, B., E. Fetzer, E. Fishbein, S.-Y. Lee, and T. Pagano, 2004: AIRS—The Atmospheric Infrared Sounder. *IGARSS 2004: 2004 IEEE Int. Geoscience and Remote Sensing Symp.*, Anchorage, AK, Institute of Electrical and Electronics Engineers, 2204–2207, https://doi.org/10.1109/IGARSS.2004.1370798.

Lamsal, L. N., B. N. Duncan, Y. Yoshida, N. A. Krotkov, K. E. Pickering, D. G. Streets, and Z. Lu, 2015: U.S. NO_2 trends (2005–2013): EPA Air Quality System (AQS) data versus improved observations from the Ozone Monitoring Instrument (OMI). *Atmos. Environ.*, **110**, 130–143, https://doi.org/10.1016/j.atmosenv.2015.03.055.

Lamsal, L. N., and Coauthors, 2021: Ozone Monitoring Instrument (OMI) Aura nitrogen dioxide standard product version 4.0 with improved surface and cloud treatments. *Atmos. Meas. Tech.*, **14**, 455–479, https://doi.org/10.5194/amt-14-455-2021.

Lange, K., and Coauthors, 2024: Validation of GEMS tropospheric NO_2 columns and their diurnal variation with ground-based DOAS measurements. *Atmos. Meas. Tech.*, **17**, 6315–6344, https://doi.org/10.5194/amt-17-6315-2024.

Lee, G. T., and Coauthors, 2024: First evaluation of the GEMS formaldehyde product against TROPOMI and ground-based column measurements during the in-orbit test period. *Atmos. Chem. Phys.*, **24**, 4733–4749, https://doi.org/10.5194/acp-24-4733-2024.

Lerot, C., and Coauthors, 2021: Glyoxal tropospheric column retrievals from TROPOMI—Multi-satellite intercomparison and ground-based validation. *Atmos. Meas. Tech.*, **14**, 7775–7807, https://doi.org/10.5194/amt-14-7775-2021.

Levelt, P. F., and Coauthors, 2018: The Ozone Monitoring Instrument: Overview of 14 years in space. *Atmos. Chem. Phys.*, **18**, 5699–5745, https://doi.org/10.5194/acp-18-5699-2018.

Li, L., and Coauthors, 2023: Improving air quality assessment using physics-inspired deep graph learning. *npj Climate Atmos. Sci.*, **6**, 152, https://doi.org/10.1038/s41612-023-00475-3.

Li, M., and Coauthors, 2024: MIXv2: A long-term mosaic emission inventory for Asia (2010–2017). *Atmos. Chem. Phys.*, **24**, 3925–3952, https://doi.org/10.5194/acp-24-3925-2024.

Li, R., and Coauthors, 2022: Representation of leaf-to-canopy radiative transfer processes improves simulation of far-red solar-induced chlorophyll fluorescence in the Community Land Model Version 5. *J. Adv. Model. Earth Syst.*, **14**, e2021MS002747, https://doi.org/10.1029/2021ms002747.

Lindsey, D. T., and Coauthors, 2024: GeoXO: NOAA's future geostationary satellite system. *Bull. Amer. Meteor. Soc.*, **105**, E660–E679, https://doi.org/10.1175/BAMS-D-23-0048.1.

Liu, F., and Coauthors, 2020: Abrupt decline in tropospheric nitrogen dioxide over China after the outbreak of COVID-19. *Sci. Adv.*, **6**, eabc2992, https://doi.org/10.1126/sciadv.abc2992.

Liu, T., L. J. Mickley, M. E. Marlier, R. S. DeFries, M. F. Khan, M. T. Latif, and A. Karambelas, 2020: Diagnosing spatial biases and uncertainties in global fire emissions inventories: Indonesia as regional case study. *Remote Sens. Environ.*, **237**, 111557, https://doi.org/10.1016/j.rse.2019.111557.

Liu, X., A. P. Mizzi, J. L. Anderson, I. Fung, and R. C. Cohen, 2021: The potential for geostationary remote sensing of NO_2 to improve weather prediction. *Atmos. Chem. Phys.*, **21**, 9573–9583, https://doi.org/10.5194/acp-21-9573-2021.

Lu, X., and Coauthors, 2021: Global methane budget and trend, 2010–2017: Complementarity of inverse analyses using in situ (GLOBALVIEWplus CH_4 ObsPack) and satellite (GOSAT) observations. *Atmos. Chem. Phys.*, **21**, 4637–4657, https://doi.org/10.5194/acp-21-4637-2021.

Ludewig, A., and Coauthors, 2020: In-flight calibration results of the TROPOMI payload on board the Sentinel-5 Precursor satellite. *Atmos. Meas. Tech.*, **13**, 3561–3580, https://doi.org/10.5194/amt-13-3561-2020.

Luo, M., H. M. Worden, R. D. Field, K. Tsigaridis, and G. S. Elsaesser, 2024: TROPESS-CrIS CO single-pixel vertical profiles: Intercomparisons with MOPITT and model simulations for 2020 western US wildfires. *Atmos. Meas. Tech.*, **17**, 2611–2624, https://doi.org/10.5194/amt-17-2611-2024.

Ma, L., D. J. Graham, and M. E. J. Stettler, 2023: Using explainable machine learning to interpret the effects of policies on air pollution: COVID-19 lockdown in London. *Environ. Sci. Technol.*, **57**, 18 271–18 281, https://doi.org/10.1021/acs.est.2c09596.

Marais, E. A., and K. Chance, 2015: A geostationary air quality monitoring platform for Africa. *Clean Air J.*, **25**, 40, https://doi.org/10.17159/2410-972X/2015/v25n1a3.

——, and C. Wiedinmyer, 2016: Air quality impact of diffuse and inefficient combustion emissions in Africa (DICE-Africa). *Environ. Sci. Technol.*, **50**, 10 739–10 745, https://doi.org/10.1021/acs.est.6b02602.

——, and Coauthors, 2012: Isoprene emissions in Africa inferred from OMI observations of formaldehyde columns. *Atmos. Chem. Phys.*, **12**, 6219–6235, https://doi.org/10.5194/acp-12-6219-2012.

——, and Coauthors, 2021: New observations of NO_2 in the upper troposphere from TROPOMI. *Atmos. Meas. Tech.*, **14**, 2389–2408, https://doi.org/10.5194/amt-14-2389-2021.

Martínez-Alonso, S., and Coauthors, 2023: S-5P/TROPOMI-derived NO_2 emissions from copper/cobalt mining and other industrial activities in the copperbelt (Democratic Republic of Congo and Zambia). *Geophys. Res. Lett.*, **50**, e2023GL104109, https://doi.org/10.1029/2023GL104109.

Mateer, C. L., D. F. Heath, and A. J. Krueger, 1971: Estimation of total ozone from satellite measurements of backscattered ultraviolet Earth radiance. *J. Atmos. Sci.*, **28**, 1307–1311, https://doi.org/10.1175/1520-0469(1971)028<1307:EOTOFS>2.0.CO;2.

Millet, D. B., D. J. Jacob, K. F. Boersma, T.-M. Fu, T. P. Kurosu, K. Chance, C. L. Heald, and A. Guenther, 2008: Spatial distribution of isoprene emissions from North America derived from formaldehyde column measurements by the OMI satellite sensor. *J. Geophys. Res.*, **113**, D02307, https://doi.org/10.1029/2007JD008950.

Miyazaki, K., and K. Bowman, 2023: Predictability of fossil fuel CO_2 from air quality emissions. *Nat. Commun.*, **14**, 1604, https://doi.org/10.1038/s41467-023-37264-8.

——, H. J. Eskes, K. Sudo, M. Takigawa, M. van Weele, and K. F. Boersma, 2012: Simultaneous assimilation of satellite NO_2, O_3, CO, and HNO_3 data for the analysis of tropospheric chemical composition and emissions. *Atmos. Chem. Phys.*, **12**, 9545–9579, https://doi.org/10.5194/acp-12-9545-2012.

——, H. Eskes, K. Sudo, K. F. Boersma, K. Bowman, and Y. Kanaya, 2017: Decadal changes in global surface NO_x emissions from multi-constituent satellite data

assimilation. *Atmos. Chem. Phys.*, **17**, 807–837, https://doi.org/10.5194/acp-17-807-2017.

——, K. W. Bowman, K. Yumimoto, T. Walker, and K. Sudo, 2020a: Evaluation of a multi-model multi-constituent assimilation framework for tropospheric chemical reanalysis. *Atmos. Chem. Phys.*, **20**, 931–967, https://doi.org/10.5194/acp-20-931-2020.

——, and Coauthors, 2020b: Updated tropospheric chemistry reanalysis and emission estimates, TCR-2, for 2005-2018. *Earth Syst. Sci. Data*, **12**, 2223–2259, https://doi.org/10.5194/essd-12-2223-2020.

——, J. L. Neu, G. Osterman, and K. Bowman, 2022: Changes in US background ozone associated with the 2011 turnaround in Chinese NO_x emissions. *Environ. Res. Commun.*, **4**, 045003, https://doi.org/10.1088/2515-7620/ac619b.

Munro, R., and Coauthors, 2016: The GOME-2 instrument on the Metop series of satellites: Instrument design, calibration, and level 1 data processing – An overview. *Atmos. Meas. Tech.*, **9**, 1279–1301, https://doi.org/10.5194/amt-9-1279-2016.

Müller, J.-F., and T. Stavrakou, 2005: Inversion of CO and NO_x emissions using the adjoint of the IMAGES model. *Atmos. Chem. Phys.*, **5**, 1157–1186, https://doi.org/10.5194/acp-5-1157-2005.

——, ——, M. Bauwens, M. George, D. Hurtmans, P. Coheur, C. Clerbaux, and C. Sweeney, 2018: Top-down CO emissions based on IASI observations and hemispheric constraints on OH levels. *Geophys. Res. Lett.*, **45**, 1621–1629, https://doi.org/10.1002/2017GL076697.

——, and Coauthors, 2024: Bias correction of OMI HCHO columns based on FTIR and aircraft measurements and impact on top-down emission estimates. *Atmos. Chem. Phys.*, **24**, 2207–2237, https://doi.org/10.5194/acp-24-2207-2024.

Oak, Y. J., and Coauthors, 2024: A bias-corrected GEMS geostationary satellite product for nitrogen dioxide using machine learning to enforce consistency with the TROPOMI satellite instrument. *Atmos. Meas. Tech.*, **17**, 5147–5159, https://doi.org/10.5194/amt-17-5147-2024.

O'Dell, K., S. Kondragunta, H. Zhang, D. L. Goldberg, G. H. Kerr, Z. Wei, B. H. Henderson, and S. C. Anenberg, 2024: Public health benefits from improved identification of severe air pollution events with geostationary satellite data. *GeoHealth*, **8**, e2023GH000890, https://doi.org/10.1029/2023GH000890.

Oomen, G.-M., and Coauthors, 2024: Weekly derived top-down volatile-organic-compound fluxes over Europe from TROPOMI HCHO data from 2018 to 2021. *Atmos. Chem. Phys.*, **24**, 449–474, https://doi.org/10.5194/acp-24-449-2024.

Park, H., and S. Jeong, 2021: Leaf area index in Earth system models: How the key variable of vegetation seasonality works in climate projections. *Environ. Res. Lett.*, **16**, 034027, https://doi.org/10.1088/1748-9326/abe2cf.

Park, J., Y. Choi, J. Jung, K. Lee, and A. K. Yeganeh, 2024: First top-down diurnal adjustment to NO_x emissions inventory in Asia informed by the Geostationary Environment Monitoring Spectrometer (GEMS) tropospheric NO_2 columns. *Sci. Rep.*, **14**, 24338, https://doi.org/10.1038/s41598-024-76223-1.

Park, S. S., J. Kim, Y. Cho, H. Lee, J. Park, D.-W. Lee, W.-J. Lee, and D.-R. Kim, 2025: Retrieval algorithm for aerosol effective height from the Geostationary Environment Monitoring Spectrometer (GEMS). *Atmos. Meas. Tech.*, https://doi.org/10.5194/amt-2023-136, in press.

Paton-Walsh, C., and Coauthors, 2022: Key challenges for tropospheric chemistry in the Southern Hemisphere. *Elementa*, **10**, 00050, https://doi.org/10.1525/elementa.2021.00050.

Pendergrass, D. C., and Coauthors, 2022: Continuous mapping of fine particulate matter ($PM_{2.5}$ air quality in East Asia at daily 6 × 6 km^2 resolution by application of a random forest algorithm to 2011–2019 GOCI geostationary satellite data. *Atmos. Meas. Tech.*, **15**, 1075–1091, https://doi.org/10.5194/amt-15-1075-2022.

——, and Coauthors, 2025: A continuous 2011–2022 record of fine particulate matter ($PM_{2.5}$) in East Asia at daily 2-km resolution from geostationary satellite observations: Population exposure and long-term trends. *Atmos. Environ.*, **346**, 121068, https://doi.org/10.1016/j.atmosenv.2025.121068.

Peuch, V.-H., and Coauthors, 2022: The Copernicus atmosphere monitoring service: From research to operations. *Bull. Amer. Meteor. Soc.*, **103**, E2650–E2668, https://doi.org/10.1175/BAMS-D-21-0314.1.

Pfister, G. G., and Coauthors, 2020: The Multi-Scale Infrastructure for Chemistry and Aerosols (MUSICA). *Bull. Amer. Meteor. Soc.*, **101**, E1743–E1760, https://doi.org/10.1175/BAMS-D-19-0331.1.

Plauchu, R., and Coauthors, 2024: NO_x emissions in France in 2019–2021 as estimated by the high-spatial-resolution assimilation of TROPOMI NO_2 observations. *Atmos. Chem. Phys.*, **24**, 8139–8163, https://doi.org/10.5194/acp-24-8139-2024.

Qu, Z., D. K. Henze, S. L. Capps, Y. Wang, X. Xu, J. Wang, and M. Keller, 2017: Monthly top-down NO_x emissions for China (2005–2012): A hybrid inversion method and trend analysis. *J. Geophys. Res. Atmos.*, **122**, 4600–4625, https://doi.org/10.1002/2016JD025852.

——, ——, N. Theys, J. Wang, and W. Wang, 2019: Hybrid mass balance/4D-Var joint inversion of NO_x and SO_2 emissions in East Asia. *J. Geophys. Res. Atmos.*, **124**, 8203–8224, https://doi.org/10.1029/2018JD030240.

——, ——, H. M. Worden, Z. Jiang, B. Gaubert, N. Theys, and W. Wang, 2022a: Sector-based top-down estimates of NO_x SO_2 and CO emissions in East Asia. *Geophys. Res. Lett.*, **49**, e2021GL096009, https://doi.org/10.1029/2021gl096009.

——, and Coauthors, 2022b: Attribution of the 2020 surge in atmospheric methane by inverse analysis of GOSAT observations. *Environ. Res. Lett.*, **17**, 094003, https://doi.org/10.1088/1748-9326/ac8754.

Riess, T. C. V. W., K. F. Boersma, J. van Vliet, W. Peters, M. Sneep, H. Eskes, and J. van Geffen, 2022: Improved monitoring of shipping NO_2 with TROPOMI: Decreasing NOx emissions in European seas during the COVID-19 pandemic. *Atmos. Meas. Tech.*, **15**, 1415–1438, https://doi.org/10.5194/amt-15-1415-2022.

Sandu, A., and T. Chai, 2011: Chemical data assimilation-An overview. *Atmosphere***2**, 426–463, https://doi.org/10.3390/atmos2030426.

Sayeed, A., and Coauthors, 2021: A novel CMAQ-CNN hybrid model to forecast hourly surface-ozone concentrations 14 days in advance. *Sci. Rep.*, **11**, 10891, https://doi.org/10.1038/s41598-021-90446-6.

Shu, L., and Coauthors, 2023: Improving ozone simulations in Asia via multi-source data assimilation: Results from an observing system simulation experiment with GEMS geostationary satellite observations. *Atmos. Chem. Phys.*, **23**, 3731–3748, https://doi.org/10.5194/acp-23-3731-2023.

Silvern, R. F., and Coauthors, 2019: Using satellite observations of tropospheric NO_2 columns to infer long-term trends in US NO_x emissions: The importance of accounting for the free tropospheric NO_2 background. *Atmos. Chem. Phys.*, **19**, 8863–8878, https://doi.org/10.5194/acp-19-8863-2019.

Sindelarova, K., S. Arellano, P. Ginoux, C. Granier, S. T. Lennartz, and D. Simpson, 2023: Natural emissions on global scale. *Handbook of Air Quality and Climate Change*, Springer Nature Singapore, 53–93, https://doi.org/10.1007/978-981-15-2760-9_7.

Soulie, A., and Coauthors, 2024: Global anthropogenic emissions (CAMS-GLOB-ANT) for the Copernicus Atmosphere Monitoring Service simulations of air quality forecasts and reanalyses. *Earth Syst. Sci. Data*, **16**, 2261–2279, https://doi.org/10.5194/essd-2023-306.

Stark, H. R., H. L. Moller, G. B. Courreges-Lacoste, R. Koopman, S. Mezzasoma, and B. Veihelmann, 2013: The Sentinel-4 mission and its implementation. *ESA Living Planet Symp.*, ESA Special Publication, 139 pp, https://ftp.spacecenter.dk/pub/Ioana/papers/s493_2star.pdf.

Stavrakou, T., J. Müller, K. F. Boersma, I. D. Smedt, and R. J. van der A, 2008: Assessing the distribution and growth rates of NO_x emission sources by inverting a 10-year record of NO_2 satellite columns. *Geophys. Res. Lett.*, **35**, L10801, https://doi.org/10.1029/2008GL033521.

——, J.-F. Müller, I. D. Smedt, M. V. Roozendael, G. R. van der Werf, L. Giglio, and A. Guenther, 2009: Global emissions of non-methane hydrocarbons deduced from SCIAMACHY formaldehyde columns through 2003–2006. *Atmos. Chem. Phys.*, **9**, 3663–3679, https://doi.org/10.5194/acp-9-3663-2009.

——, and Coauthors, 2012: Satellite evidence for a large source of formic acid from boreal and tropical forests. *Nat. Geosci.*, **5**, 26–30, https://doi.org/10.1038/ngeo1354.

——, J.-F. Müller, M. Bauwens, I. D. Smedt, M. V. Roozendael, and A. Guenther, 2018: Impact of short-term climate variability on volatile organic compounds emissions assessed using OMI satellite formaldehyde observations. *Geophys. Res. Lett.*, **45**, 8681–8689, https://doi.org/10.1029/2018GL078676.

——, ——, ——, K. F. Boersma, and J. van Geffen, 2020: Satellite evidence for changes in the NO_2 weekly cycle over large cities. *Sci. Rep.*, **10**, 10066, https://doi.org/10.1038/s41598-020-66891-0.

Streets, D. G., and Coauthors, 2013: Emissions estimation from satellite retrievals: A review of current capability. *Atmos. Environ.*, **77**, 1011–1042, https://doi.org/10.1016/j.atmosenv.2013.05.051.

Sun, K., and Coauthors, 2018: A physics-based approach to oversample multi-satellite, multispecies observations to a common grid. *Atmos. Meas. Tech.*, **11**, 6679–6701, https://doi.org/10.5194/amt-11-6679-2018.

Tang, W., and Coauthors, 2021: Assessing sub-grid variability within satellite pixels over urban regions using airborne mapping spectrometer measurements. *Atmos. Meas. Tech.*, **14**, 4639–4655, https://doi.org/10.5194/amt-14-4639-2021.

——, and Coauthors, 2023: Application of the multi-scale infrastructure for chemistry and aerosols version 0 (MUSICAv0) for air quality research in Africa. *Geosci. Model Dev.*, **16**, 6001–6028, https://doi.org/10.5194/gmd-16-6001-2023.

Tang, X., and Coauthors, 2013: Inversion of CO emissions over Beijing and its surrounding areas with ensemble Kalman filter. *Atmos. Environ.*, **81**, 676–686, https://doi.org/10.1016/j.atmosenv.2013.08.051.

Taylor, I. A., J. Preston, E. Carboni, T. A. Mather, R. G. Grainger, N. Theys, S. Hidalgo, and B. M. Kilbride, 2018: Exploring the utility of IASI for monitoring volcanic SO_2 emissions. *J. Geophys. Res. Atmos.*, **123**, 5588–5606, https://doi.org/10.1002/2017JD027109.

Theys, N., and Coauthors, 2020: Global nitrous acid emissions and levels of regional oxidants enhanced by wildfires. *Nat. Geosci.*, **13**, 681–686, https://doi.org/10.1038/s41561-020-0637-7.

——, and Coauthors, 2021: A sulfur dioxide Covariance-Based Retrieval Algorithm (COBRA): Application to TROPOMI reveals new emission sources. *Atmos. Chem. Phys.*, **21**, 16 727–16 744, https://doi.org/10.5194/acp-21-16727-2021.

Tilstra, L. G., M. de Graaf, V. J. H. Trees, P. Litvinov, O. Dubovik, and P. Stammes, 2024: A directional surface reflectance climatology determined from TROPOMI observations. *Atmos. Meas. Tech.*, **17**, 2235–2256, https://doi.org/10.5194/amt-17-2235-2024.

Timmermans, R., and Coauthors, 2019: Impact of synthetic space-borne NO_2 observations from the Sentinel-4 and Sentinel-5P missions on tropospheric NO_2 analyses. *Atmos. Chem. Phys.*, **19**, 12 811–12 833, https://doi.org/10.5194/acp-19-12811-2019.

Torres, O., P. K. Bhartia, H. Jethva, and C. Ahn, 2018: Impact of the ozone monitoring instrument row anomaly on the long-term record of aerosol products. *Atmos. Meas. Tech.*, **11**, 2701–2715, https://doi.org/10.5194/amt-11-2701-2018.

——, H. Jethva, C. Ahn, G. Jaross, and D. G. Loyola, 2020: TROPOMI aerosol products: Evaluation and observations of synoptic-scale carbonaceous aerosol plumes during 2018–2020. *Atmos. Meas. Tech.*, **13**, 6789–6806, https://doi.org/10.5194/amt-13-6789-2020.

Valin, L. C., A. R. Russell, and R. C. Cohen, 2013: Variations of OH radical in an urban plume inferred from NO_2 column measurements. *Geophys. Res. Lett.*, **40**, 1856–1860, https://doi.org/10.1002/grl.50267.

Valmassoi, A., and Coauthors, 2023: Current challenges and future directions in data assimilation and reanalysis. *Bull. Amer. Meteor. Soc.*, **104**, E756–E767, https://doi.org/10.1175/BAMS-D-21-0331.1.

Van Damme, M., S. Whitburn, L. Clarisse, C. Clerbaux, D. Hurtmans, and P.-F. Coheur, 2017: Version 2 of the IASI NH_3 neural network retrieval algorithm: Near-real-time and reanalysed datasets. *Atmos. Meas. Tech.*, **10**, 4905–4914, https://doi.org/10.5194/amt-10-4905-2017.

——, L. Clarisse, S. Whitburn, J. Hadji-Lazaro, D. Hurtmans, C. Clerbaux, and P.-F. Coheur, 2018: Industrial and agricultural ammonia point sources exposed. *Nature*, **564**, 99–103, https://doi.org/10.1038/s41586-018-0747-1.

van der A, R. J., A. T. J. de Laat, J. Ding, and H. J. Eskes, 2020: Connecting the dots: NO_x emissions along a West Siberian natural gas pipeline. *npj Climate Atmos. Sci.*, **3**, 16, https://doi.org/10.1038/s41612-020-0119-z.

——, J. Ding, and H. Eskes, 2024: Monitoring European anthropogenic NO_x emissions from space. *Atmos. Chem. Phys.*, **24**, 7523–7534, https://doi.org/10.5194/acp-24-7523-2024.

van der Graaf, S., E. Dammers, A. Segers, R. Kranenburg, M. Schaap, M. W. Shephard, and J. W. Erisman, 2022: Data assimilation of CrIS NH_3 satellite observations for improving spatiotemporal NH_3 distributions in LOTOS-EUROS. *Atmos. Chem. Phys.*, **22**, 951–972, https://doi.org/10.5194/acp-22-951-2022.

van Geffen, J., and Coauthors, 2022: Sentinel-5P TROPOMI NO_2 retrieval: Impact of version v2.2 improvements and comparisons with OMI and ground-based data. *Atmos. Meas. Tech.*, **15**, 2037–2060, https://doi.org/10.5194/amt-15-2037-2022.

Varon, D. J., D. J. Jacob, J. McKeever, D. Jervis, B. O. A. Durak, Y. Xia, and Y. Huang, 2018: Quantifying methane point sources from fine-scale satellite observations of atmospheric methane plumes. *Atmos. Meas. Tech.*, **11**, 5673–5686, https://doi.org/10.5194/amt-11-5673-2018.

Veefkind, J. P., J. de Haan, E. Brinksma, M. Kroon, and P. Levelt, 2006: Total ozone from the ozone monitoring instrument (OMI) using the DOAS technique. *IEEE Trans. Geosci. Remote Sens.*, **44**, 1239–1244, https://doi.org/10.1109/TGRS.2006.871204.

Veefkind, J. P., and Coauthors, 2012: TROPOMI on the ESA Sentinel-5 Precursor: A GMES mission for global observations of the atmospheric composition for climate, air quality and ozone layer applications. *Remote Sens. Environ.*, **120**, 70–83, https://doi.org/10.1016/j.rse.2011.09.027.

Vu Van, A., and Coauthors, 2023: Near-real-time detection of unexpected atmospheric events using principal component analysis on the Infrared Atmospheric Sounding Interferometer (IASI) radiances. *Atmos. Meas. Tech.*, **16**, 2107–2127, https://doi.org/10.5194/amt-16-2107-2023.

Wang, J. S., S. R. Kawa, G. J. Collatz, M. Sasakawa, L. V. Gatti, T. Machida, Y. Liu, and M. E. Manyin, 2018: A global synthesis inversion analysis of recent variability in CO_2 fluxes using GOSAT and in situ observations. *Atmos. Chem. Phys.*, **18**, 11 097–11 124, https://doi.org/10.5194/acp-18-11097-2018.

Wang, M., X. Chen, Z. Jiang, T.-L. He, D. Jones, J. Liu, and Y. Shen, 2024: Meteorological and anthropogenic drivers of surface ozone change in the north China plain in 2015–2021. *Sci. Total Environ.*, **906**, 167763, https://doi.org/10.1016/j.scitotenv.2023.167763.

Wang, Y., and X. Wang, 2023: Simultaneous multiscale data assimilation using scale- and variable-dependent localization in EnVar for convection allowing analyses and forecasts: Methodology and experiments for a tornadic supercell. *J. Adv. Model. Earth Syst.*, **15**, e2022MS003430, https://doi.org/10.1029/2022MS003430.

——, J. Wang, X. Xu, D. K. Henze, Z. Qu, and K. Yang, 2020: Inverse modeling of SO_2 and NO_x emissions over China using multisensor satellite data – Part 1: Formulation and sensitivity analysis. *Atmos. Chem. Phys.*, **20**, 6631–6650, https://doi.org/10.5194/acp-20-6631-2020.

——, G. P. Brasseur, and T. Wang, 2022: Segregation of atmospheric oxidants in turbulent urban environments. *Atmosphere*, **13**, 315, https://doi.org/10.3390/atmos13020315.

Watine-Guiu, M., D. J. Varon, I. Irakulis-Loitxate, N. Balasus, and D. J. Jacob, 2023: Geostationary satellite observations of extreme and transient methane emissions from oil and gas infrastructure. *Proc. Natl. Acad. Sci. USA*, **120**, e2310797120, https://doi.org/10.1073/pnas.2310797120.

Wei, J., and Coauthors, 2020: Improved 1 km resolution $PM_{2.5}$ estimates across China using enhanced space–time extremely randomized trees. *Atmos. Chem. Phys.*, **20**, 3273–3289, https://doi.org/10.5194/acp-20-3273-2020.

Wells, K. C., and Coauthors, 2020: Satellite isoprene retrievals constrain emissions and atmospheric oxidation. *Nature*, **585**, 225–233, https://doi.org/10.1038/s41586-020-2664-3.

——, and Coauthors, 2022: Next-generation isoprene measurements from space: Detecting daily variability at high resolution. *J. Geophys. Res. Atmos.*, **127**, e2021JD036181, https://doi.org/10.1029/2021JD036181.

——, and Coauthors, 2025: Global decadal measurements of methanol, ethene, ethyne, and HCN from the Cross-track Infrared Sounder. *Atmos. Meas. Tech.*, **18**, 695–716, https://doi.org/10.5194/amt-18-695-2025.

West, J. J., and Coauthors, 2013: Co-benefits of mitigating global greenhouse gas emissions for future air quality and human health. *Nat. Climate Change*, **3**, 885–889, https://doi.org/10.1038/NCLIMATE2009.

Whitburn, S., and Coauthors, 2016: A flexible and robust neural network IASI-NH3 retrieval algorithm. *J. Geophys. Res. Atmos.*, **121**, 6581–6599, https://doi.org/10.1002/2016JD024828.

Wiedinmyer, C., R. J. Yokelson, and B. K. Gullett, 2014: Global emissions of trace gases, particulate matter, and hazardous air pollutants from open burning of domestic waste. *Environ. Sci. Technol.*, **48**, 9523–9530, https://doi.org/10.1021/es502250z.

Wright, C. J., and Coauthors, 2022: Surface-to-space atmospheric waves from Hunga Tonga–Hunga Ha'apai eruption. *Nature*, **609**, 741–746, https://doi.org/10.1038/s41586-022-05012-5.

Yang, D., J. Hakkarainen, Y. Liu, I. Ialongo, Z. Cai, and J. Tamminen, 2023a: Detection of anthropogenic CO_2 emission signatures with TanSat CO_2 and with Copernicus Sentinel-5 Precursor (S5P) NO_2 measurements: First results. *Adv. Atmos. Sci.*, **40**, 1–5, https://doi.org/10.1007/s00376-022-2237-5.

Yang, J., Z. Zhang, C. Wei, F. Lu, and Q. Guo, 2017: Introducing the new generation of Chinese geostationary weather satellites, Fengyun-4. *Bull. Amer. Meteor. Soc.*, **98**, 1637–1658, https://doi.org/10.1175/BAMS-D-16-0065.1.

Yang, L. H., and Coauthors, 2023b: Tropospheric NO_2 vertical profiles over South Korea and their relation to oxidant chemistry: Implications for geostationary satellite retrievals and the observation of NO_2 diurnal variation from space. *Atmos. Chem. Phys.*, **23**, 2465–2481, https://doi.org/10.5194/acp-23-2465-2023.

Yumimoto, K., I. Uno, and S. Itahashi, 2014: Long-term inverse modeling of Chinese CO emission from satellite observations. *Environ. Pollut.*, **195**, 308–318, https://doi.org/10.1016/j.envpol.2014.07.026.

Zeng, Z.-C., L. Lee, and C. Qi, 2023a: Diurnal carbon monoxide observed from a geostationary infrared hyperspectral sounder: First result from GIIRS on board FengYun-4B. *Atmos. Meas. Tech.*, **16**, 3059–3083, https://doi.org/10.5194/amt-16-3059-2023.

——, ——, ——, L. Clarisse, and M. Van Damme, 2023b: Optimal estimation retrieval of tropospheric ammonia from the geostationary interferometric infrared sounder on board FengYun-4B. *Atmos. Meas. Tech.*, **16**, 3693–3713, https://doi.org/10.5194/amt-16-3693-2023.

——, B. Franco, L. Clarisse, L. Lee, C. Qi, and F. Lu, 2024: Observing a volatile organic compound from a geostationary infrared sounder: HCOOH from FengYun-4B/GIIRS. *J. Geophys. Res. Atmos.*, **129**, e2024JD041352, https://doi.org/10.1029/2024JD041352.

Zhang, B., and Coauthors, 2023: Machine learning assesses drivers of $PM_{2.5}$ air pollution trend in the Tibetan Plateau from 2015 to 2022. *Sci. Total Environ.*, **878**, 163189, https://doi.org/10.1016/j.scitotenv.2023.163189.

Zhang, H., Z. Wei, B. H. Henderson, S. C. Anenberg, K. O'Dell, and S. Kondragunta, 2022: Nowcasting applications of geostationary satellite hourly surface $PM_{2.5}$ data. *Wea. Forecasting*, **37**, 2313–2329, https://doi.org/10.1175/waf-d-22-0114.1.

Zheng, B., and Coauthors, 2018: Trends in China's anthropogenic emissions since 2010 as the consequence of clean air actions. *Atmos. Chem. Phys.*, **18**, 14095–14111, https://doi.org/10.5194/acp-18-14095-2018.

——, and Coauthors, 2019: Global atmospheric carbon monoxide budget 2000–2017 inferred from multi-species atmospheric inversions. *Earth Syst. Sci. Data*, **11**, 1411–1436, https://doi.org/10.5194/essd-11-1411-2019.

Zoogman, P., and Coauthors, 2017: Tropospheric emissions: Monitoring of pollution (TEMPO). *J. Quant. Spectrosc. Radiat. Transfer*, **186**, 17–39, https://doi.org/10.1016/j.jqsrt.2016.05.008.

Zuo, X., and Coauthors, 2023: Observing downwind structures of urban HCHO plumes from space: Implications to non-methane volatile organic compound emissions. *Geophys. Res. Lett.*, **50**, e2023GL106062, https://doi.org/10.1029/2023GL106062.